Hysteresis Patterns of Watershed Nitrogen Retention and Loss over the past 50 years in United States Hydrological Basins

*Michelle E. Newcomer[1], Nicholas J Bouskill[1], Haruko Wainwright[1], Taylor Maavara[2], Bhavna Arora[1], Erica R. Siirila-Woodburn[1], Dipankar Dwivedi[1], Ken Williams[1], Carl Steefel[1], Susan S. Hubbard[1]

[1]Lawrence Berkeley National Lab, Earth & Environmental Sciences Area

[2]Yale University, School of the Environment

*Corresponding author: M. Newcomer, mnewcomer@lbl.gov

Key Points:

- Declines in nitrogen (N) exports were documented in 34% of the USGS monitoring stations distributed throughout the CONUS, in areas with increasing N deposition and increasing vegetation health/density patterns
- Watershed N retention undergoing reversal from N saturation displays both unique hysteresis (recovery) patterns and one-way transition patterns to new steady states
- Atmospheric deposition and vegetation productivity/biomass explain up to 45% of the variability in watershed N retention trends
- Land use trends explain the least amount of variability (<10%) of watershed N retention trends

Index Terms: Water quality, Nutrient exports, Watershed Responses

Keywords: Watersheds, Nitrogen dynamics, ecosystem variability, catchment scale nitrogen retention, watershed exports

Abstract

Patterns of watershed nitrogen (N) retention and loss are shaped by how watershed biogeochemical processes retain, biogeochemically transform, and lose incoming atmospheric deposition of N. Loss patterns represented by concentration, discharge, and their associated stream exports are important indicators of watershed N retention patterns because they reveal hysteresis patterns (i.e. return to initial state) or one-way transition patterns (i.e. new steady state) that provide insight into watershed conditions driving long term stream trends. We examined the degree to which Continental U.S. (CONUS) scale deposition patterns (wet and dry atmospheric deposition), vegetation trends, and stream trends can be potential indicators of watershed N-saturation and retention conditions, and how watershed N retention and losses vary over space and time. By synthesizing changes and modalities in watershed nitrogen loss patterns based on stream data from 2200 U.S. watersheds over a 50 year record, our work characterized a new hysteresis conceptual model based on factors driving watershed N-retention and loss, including hydrology, atmospheric inputs, land-use, stream temperature, elevation, and vegetation. Our results show that atmospheric deposition and vegetation productivity groups that have strong positive or negative trends over time are associated with patterns of stream loss that uniquely indicate the stage of watershed N-saturation and reveal unique characteristics of watershed N-

retention hysteresis patterns. In particular, regions with increasing atmospheric deposition and increasing vegetation health/biomass patterns have the highest N-retention capacity, become increasingly N-saturated over time, and are associated with the strongest declines in stream N exports—a pattern that is consistent across all land cover categories. In particular, the second largest factor explaining watershed N-retention was in-stream temperature and dissolved organic carbon concentration trends, while land-use explained the least amount of variability in watershed N-retention. Our CONUS scale investigation supports an updated hysteresis conceptual model of watershed N-retention and loss, providing great value to using long-term stream monitoring data as indicators of watershed N hysteresis patterns.

1.0 Introduction

Watershed stream concentrations of nitrogen (N) and carbon (C), and hydrological connectivity driving exports of N and C to coastal zones have been changing around the world. Changes in N and C concentrations and exports (concentration x discharge) are often linked to a variety of direct and indirect causes at watershed scales, many of which examine the degree to which watersheds can retain N (Aber et al., 1998; Bernal et al., 2012; Crawford et al., 2019; Musolff et al., 2016; Smith et al., 1987; Stoddard, 1994; Vuorenmaa et al., 2018). Recent studies indicate that N and C watershed exports have both increased and decreased in watersheds across the continental United States (CONUS) over the last 50 years (Driscoll et al., 2003; Hale et al., 2015; Oelsner et al., 2017; Oelsner & Stets, 2019; Shoda et al., 2019). To explain these trends, studies often point to ecosystems recovering from acidic deposition (Lawrence et al., 2020; Stoddard et al., 1999), recovery from atmospheric N-deposition (Eshleman et al., 2013; Kothawala et al., 2011), watershed management (J. Murphy & Sprague, 2019), and agricultural

practices (Renwick et al., 2018; Van Meter & Basu, 2015). Because the watershed biogeochemical characteristics controlling N and C retention, cycling, and loss are a non-linear function of N-deposition, many diverse hypotheses focused on both natural and anthropogenic processes exist to explain trends of in-stream N and C conditions and exports and associated watershed N-retention (Aber et al., 1998; Bernhardt et al., 2005; Guo et al., 2019; Marinos et al., 2018; Stoddard, 1994). Despite the many existing studies examining controls on watershed N retention and loss at regional scales, a comprehensive analysis examining the co-occurrence of watershed N-retention and stream loss patterns has yet to emerge.

An important anthropogenic process directly linked to watershed in-stream concentrations of N and C is atmospheric N-deposition. Around the world, atmospheric deposition of N has increased since the industrial revolution (Pinder et al., 2012). Despite air pollution management regulations that have led to declining atmospheric N-deposition trends in some regions (Li et al., 2016), long term N-addition to watersheds has significantly altered the N-retention capacity of watersheds. Specifically, N-retention capacity is the ability to store, retain, or cycle N within the watershed. Retention is balanced by storage and biogeochemical cycling mechanisms that determine release of N which is exported via streams (Stoddard, 1994). N-saturation is a condition whereby N-inputs exceed the biogeochemical retention capacity of the system to release, cycle, store, or retain N within living biomass (plants or microbes) or abiotic ecosystem components (e.g. soils). Once N-saturated conditions are reached, variable rates of C and N release to streams can occur (Pardo et al., 2011). The role of N-deposition on watershed retention of N and release to streams is an ongoing area of research complicated by both terrestrial and aquatic mechanisms.

Indeed, much of the debate over whether stream N is a function of atmospheric N deposition is centered on the degree to which watersheds can either retain and release N through biotic and abiotic factors (Aber et al., 2003; Lovett et al., 2000; Stoddard, 1994). Foundational nitrogen studies have hypothesized that alleviation of nitrogen limitation in soils have led to increased nitrate mobility, positive effects on vegetation productivity (Aber et al., 1998), and subsequent mobilization of nitrogen to streams (Stoddard, 1994). Once inputs surpass biological demand, the watershed may become N-saturated, and additional supply may lead to vegetation mortality through decreased cation availability (Lucas et al., 2011; Shultz et al., 2018), enhancing N transport through nitrification and mineralization. Observations of decadal declines in N concentrations and exports in streams despite increased N-deposition have confounded many of these foundational ideas (Goodale et al., 2003; Lucas et al., 2016). More recently however, significant reductions atmospheric N deposition in some regions have reinvigorated research around this topic because of the opportunity afforded by this natural experiment to test these hypotheses (Eshleman et al., 2013).

Observations of trends in watershed N and C exports and concentration in streams have been proposed as potential indicators of watershed N-retention status because stream exports relate to landscape release patterns as indirect measurements of those same processes (Goodale et al., 2005). An extensive body of research has examined such stream measurements at regional-scales. Multi-decadal trends in surface water solute chemistry and exports of dissolved organic carbon (DOC) and dissolved inorganic nitrogen (DIN) have been identified as a function of watershed characteristics, climate, and anthropogenic factors (Ballard et al., 2019; Bellmore et al., 2018; Boyer et al., 2006; Moatar et al., 2017; Musolff et al., 2015; Oelsner & Stets, 2019; Shoda et al., 2019; Stoddard et al., 1999; Zarnetske et al., 2018). Many studies have examined

the role of atmospheric N-deposition (Driscoll et al., 2003; Monteith et al., 2007; Musolff et al., 2017; Stoddard et al., 1999, 2016). The role of changing atmospheric loading on watershed N retention is confounded by other hydrobiogeochemical and landscape variables including geology, vegetation, soil characteristics, microbial communities, land cover/land use, climate, wetland cover (e.g. (Aber et al., 2003; Bellmore et al., 2018; Boyer et al., 2006; Stoddard, 1994)) as well as disturbances, such as wildfire (Jensen et al., 2017; S. F. Murphy et al., 2015; Rhoades et al., 2018). Because atmospherically deposited N is involved in range of biotic and abiotic transformations and redox cycling before reaching the stream, stream DIN and DOC exports may either deviate from or mirror atmospheric deposition trends (Argerich et al., 2013; Bernal et al., 2012; Halliday et al., 2013; Lovett et al., 2000; Musolff et al., 2015; SanClements et al., 2018).

A suite of mechanistic biogeochemical controls in the landscape have been identified as factors relating watershed N-retention to stream exports. Addition of N on the landscape has been documented to impact the following mechanisms: soil microbial mineralization/immobilization, and abiotic immobilization (Goodale et al., 2005; Huntington, 2005; Lovett et al., 2018), biotic uptake (Goodale et al., 2005; Huntington, 2005; Yanai et al., 2013), declining organic matter decomposition (Bowden et al., 2019; Janssens et al., 2010), shifting soil C:N ratios (Groffman et al., 2018; Yanai et al., 2013) leading to specific thresholding behavior for N release to streams (Evans et al., 2006), and altered soil organic carbon composition (Bowden et al., 2019; Evans et al., 2006) including declines in the rapidly cycling labile carbon pools (Cusack et al., 2011). In addition, complex internal soil mechanisms responding to increasing atmospheric CO_2 have been found to drive increased N retention and soil carbon cycling limiting stocks of labile organic carbon (Groffman et al., 2018; Hungate et al., 1997; Huntington, 2005).

Once N and C reach the stream, additional biogeochemical mechanisms exist that impact stream exports. In-stream response to variable DOC lability (Groffman et al., 2018; O'Donnell et al., 2010) can impact in-stream and hyporheic denitrification (Goodale et al., 2005) tilting streams towards thermodynamic limitations (e.g. monomeric and polymeric carbon) rather than kinetic limitations (e.g. concentration) (Garayburu-Caruso et al., 2020; Stegen et al., 2018). The pool of C and N that reaches the stream is also determined by hydrological conditions that shift stream water from fast to slow flow paths (i.e. runoff and infiltration partitioning). Deeper flows can access more aged, microbially sourced carbon pools (nonaromatic, recalcitrant), while more shallow flows access more young terrestrially derived carbon from vegetation and soils (Barnes et al., 2018). Given that shifts in precipitation are expected to be the dominant driver of changes in partitioning of runoff and infiltration as primary sources of water to streams (difference between young versus older water), as well as evapotranspiration drivers of water table fluctuations, changes in hydrology are quite likely to affect flow paths and access to different sources of carbon of varying characteristics. Regionally, even slightly dryer conditions or greater evapotranspiration can lead to deeper flow paths and longer residence times providing access to legacy nitrogen sources which would increase watershed exports despite little to no change in discharge. Legacy nitrogen is a potentially confounding variable that may impact direct analysis of watershed retention (Van Meter et al., 2016; Van Meter & Basu, 2015).

Despite these complexities discussed above, conceptual models examining connections between soil, atmospheric, vegetation, and stream water trends as indicators of and responses to deposition conditions have significantly advanced understanding of watershed response to decadal atmospheric N addition. Such conceptual models have identified many trajectories for landscape evolution after decades of atmospheric N deposition—watersheds may either return to

the initial state after the perturbation (hysteresis), or transition to a new stable state (one-way transition) (Aber et al., 1998; Lovett et al., 2018; Vitousek & Reiners, 1975). Hysteresis in this sense refers to the recovery of the watershed to the original state, but through a different path. More recent conceptual models include previously unrecognized mechanisms related to soil N re-accumulation and storage (Lovett et al., 2018; Lovett & Goodale, 2011) and loss of base cations within soil (Lawrence et al., 2020). Observations of decadal long stream N and C hysteresis patterns, driven in some cases by state shifts between interacting soil mycorrhizal, microbial and plant communities after N deposition declines, point to the potential for biotic and abiotic conditions within watersheds to either reach a new equilibrium state or display hysteresis under declining N-deposition (i.e. recovery) (Gilliam et al., 2019). While these recent studies have advanced new conceptual models at the regional scale, they have yet to be tested against CONUS scale trends relative to watershed inputs and outputs. New insights and conceptual models will be needed to frame these stream trends in the context of important watershed characteristics and the vast amount of aquatic and terrestrial data available (Figure 1).

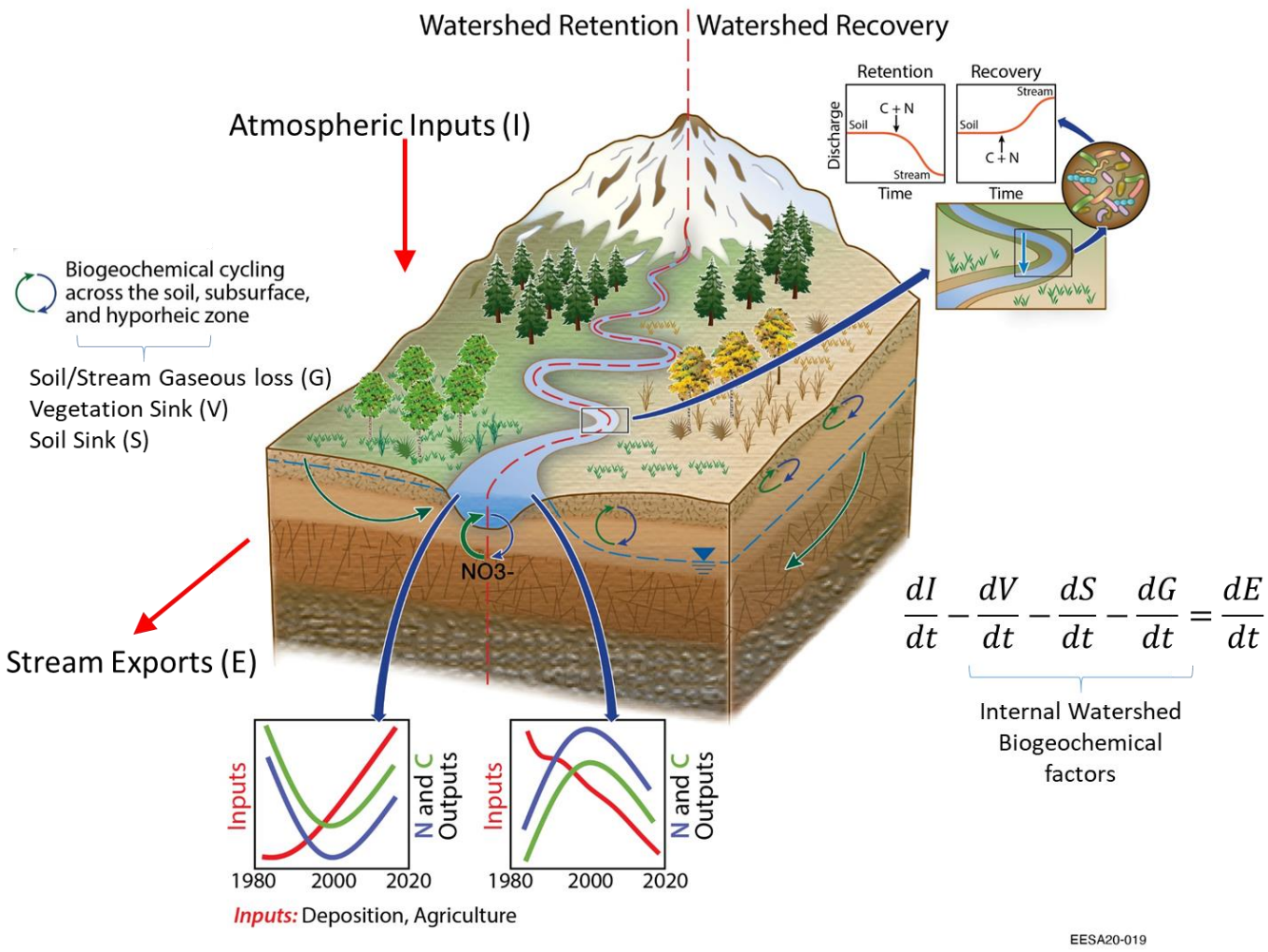

176

177 Figure 1: Hydro-biogeochemical processes occurring from bedrock to canopy and across
178 elevation gradients influence the retention and transformation of input atmospheric N deposition
179 (*I*), leading to distinct export signatures (*E*). During the progressive stages of atmospheric
180 deposition of N, watersheds have the capacity to retain N through various soil and vegetation
181 sink terms, and biogeochemical processes leading to reduced C and N delivery to streams, and
182 export patterns unique to the 'watershed retention' stage (left side of watershed). During the
183 recessive stage of atmospheric deposition, 'watershed recovery' occurs from decreased
184 atmospheric deposition loadings, and watersheds exhibit unique patterns of stream export in
185 response to greater movement of C and N from soils to stream (right side of watershed). The

186 watershed equation is modified from Lovett & Goodale (2011) where *dI/dt* is the Input rate,
187 *dV/dt* is the rate of vegetation uptake, *dS/dt* is the soil sink rate, dG/dt is the soil and stream
188 gaseous loss rate, and *dE/dt* is the stream export rate. Inputs, vegetation, and exports were all
189 evaluated at the yearly and seasonal time scales.
190
191 In the present study, we examine the degree to which CONUS scale atmospheric deposition
192 patterns, vegetation trends, and stream trends can potentially be indicators of watershed N-
193 saturation, retention, and recovery conditions. We also examine how watershed N retention and
194 losses vary over space and time. In this work we define watershed N losses as the stream export
195 term, atmospheric deposition as the input term, and the difference between inputs and losses
196 being equal to the internal soil, vegetative, and gaseous biogeochemical cycling terms (i.e. soil
197 and aquatic denitrification) (Eshleman et al., 2013). We do not directly analyze internal
198 biogeochemical cycling terms in this study (i.e. soil and aquatic denitrification, gaseous loss), but
199 we use knowledge of these mechanisms from many prior studies to help develop our conceptual
200 model. Our four stage hysteresis conceptual model of N-saturation and associated stream exports
201 allows for reversal and recovery (i.e. hysteresis) or complete transition to a new stable steady
202 state following the combined factors including atmospheric deposition trends, vegetation trends
203 represented by remote-sensing measurements of NDVI, and stream conditions to explain trends
204 (Lovett et al., 2000). With a reversal of N-deposition reported, we hypothesize this conceptual
205 model will account for the wide variety of observed N concentration and export trends.
206 The four groups that are hypothesized to contribute to N and C export as a function of
207 atmospheric N-deposition and vegetation NDVI trends are depicted in Figure 2:

- Group a, Retention: Retention capacity is at its highest (can retain most of incoming N deposition). Watershed retention of incoming N deposition is close to 100% indicated by small watershed exports relative to deposition. This group is represented by locations where total atmospheric N deposition and vegetation health/biomass indices (represented by Normalized Difference Vegetation Index, NDVI) are increasing, leading to elevated N retention. Stream exports of N and C decline due to net immobilization in soils, high stream denitrification and biological uptake from more thermodynamically favorable (more labile) carbon delivered to the stream and produced in the stream from photoautotrophs. These watersheds have not yet reached N-saturation loosely quantified by soil C/N molar ratios that are > 40 (Evans et al., 2006).
- Group b, Saturation: Retention capacity is still at its highest but approaching saturated conditions. Watershed retention of incoming N deposition is close to 100% indicated by small watershed exports relative to deposition, and some watersheds may indicate saturated conditions by showing declines in retention through increasing export trends. This group is represented by locations where total N-deposition continues to increase over time, but vegetation biomass/productivity indices decline (negative NDVI trends). These watersheds generally show soil C/N ratios that are < 40. While N immobilization slows as biotic and abiotic stores become saturated, C and N delivery to streams is limited because landscape retention is still occurring. Moreover, continued stream denitrification leads to a lack of any obvious saturation or trend signal in water quality, accompanied by observations of predominant decreasing trends of riverine nitrogen, albeit with some increasing trends in DIN and labile DOC.

- Group c, Release: As watersheds undergo regional declines in atmospheric N deposition after experiencing periods of elevated atmospheric N deposition, vegetation biomass/productivity indices improve (positive NDVI trends), soils remain saturated in N relative to C, and N release from soils to streams continues. Even though leaching of N and organic matter to streams increases due to saturated conditions, immobilization and deeper N storage within soil horizons may continue but at a greatly declining rate depending on soil biotic/abiotic/microbial processes. Carbon begins to shift to a less thermodynamically favorable state (less labile) thereby limiting in-stream microbial denitrification, leading an increase in C export. In some locations it would be expected that stream exports of N increase because of the reduced capacity for soil N storage and from limited denitrification.
- Group d, Recovery: In the final stage of reversal from N-deposition, vegetation health indices show some signs of decline because of a return to N limiting conditions, soil provisions of N and C to the stream begin to increase as soil immobilization plateaus and C/N ratios rise above 40. Even though soil C and N delivery to streams continues, continued decline of thermodynamically favorable carbon to streams limits denitrification potential and allows for continuous increases in stream exports of N.

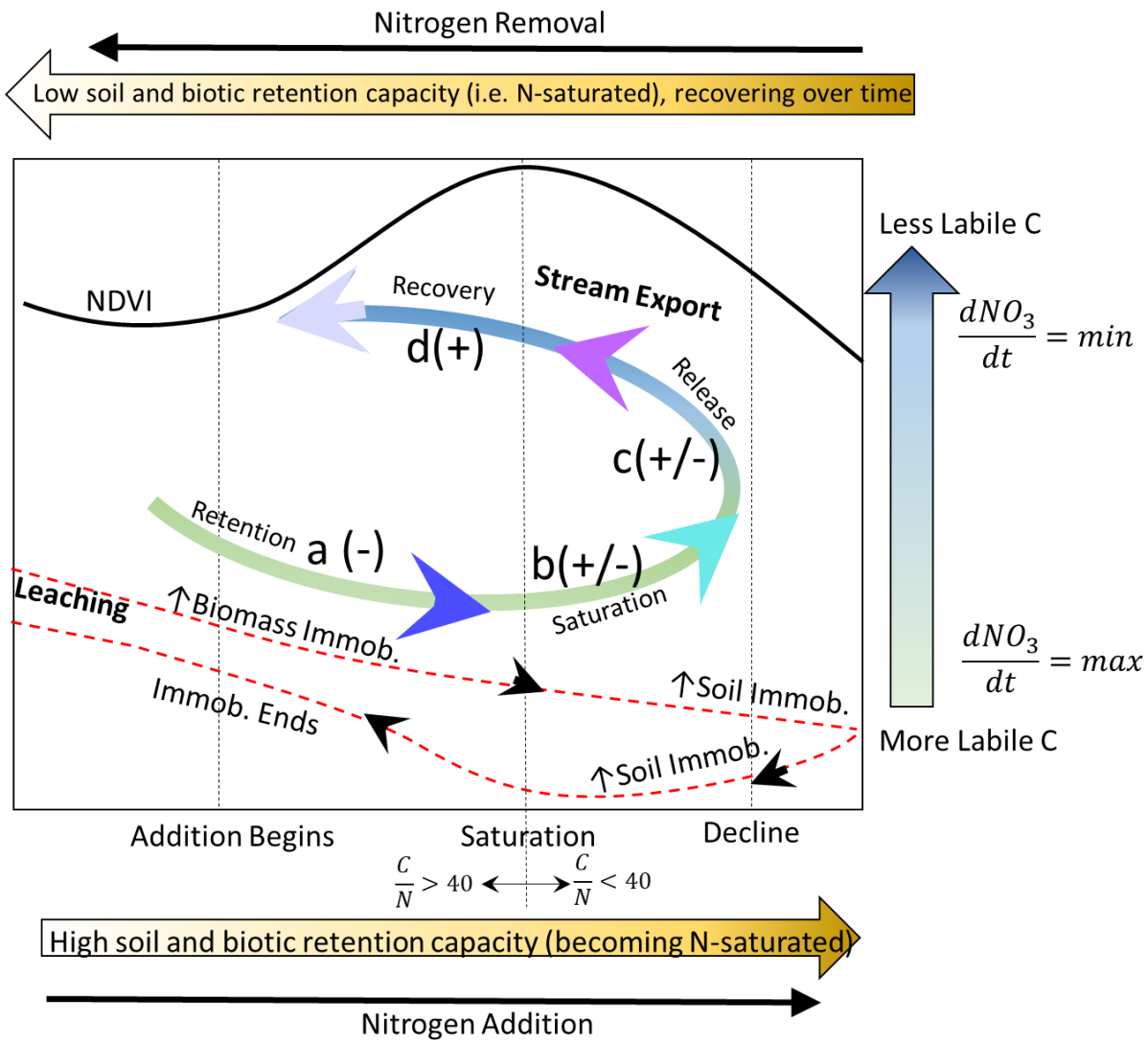

Figure 2: Our updated conceptual model of responses to N-saturation within watersheds showing the hysteresis pattern of N exports moving from retention to recovery. Figure modified from concepts described by Aber and Stoddard in prior studies (Aber et al., 1998; Stoddard, 1994) and others (Gilliam et al., 2019). The groupings a, b, c, and d, represent different stages on the hypothesized hysteresis curve of vegetation and NO_3 delivery response to N-deposition referenced in-text below. Group a should show a decline in stream exports (as indicated by '-'), Groups b and c show variable (+/-) stream exports depending on the other conditions, and Group d should show increases (+) in stream exports. Leaching, the process of soil delivery of N and C

to streams is shown by the red dashed line and is represented as a function of soil and biomass immobilization. While immobilization occurs, leaching is reduced until immobilization ends.

Using the conceptual model outlining N-dynamics illustrated in Figure 2, our goal is to identify and quantify watershed N retention conditions, hysteresis patterns, and transitions across the CONUS using stream concentration and export indicators. The knowledge gaps related to watershed N-retention highlighted above motivate three research questions that we address: 1) How are in-stream N and C concentrations (*Cn*) and exports *(Ex)* changing, both annually and seasonally, and how do these changes relate to discharge (*Qs*), vegetation, land-use, and atmospheric N deposition? 2) Do stream water quality trends support the hypothesized groups of watershed N-retention and provide evidence for hysteresis patterns? 3) Can groups of changing TDEP and NDVI provide insight into hydro-biogeochemical processes controlling watershed export trends and watershed N-retention hysteresis or one-way transition patterns? We conduct this work over the CONUS scale to quantify and track where retention patterns are changing, and to provide conceptual guidance for large scale controlling factors on these trends including the role of deposition, vegetation, land-use, and in-stream conditions.

To evaluate how watersheds across the US have responded to changes in depositional trends, we calculate decadal trends in stream concentrations and exports of C and N such as dissolved inorganic nitrogen (DIN) and dissolved organic carbon (DOC). We examine five variables of interest that are available at the CONUS scale and that represent controls on in-stream DIN concentrations and exports: net (wet+dry) atmospheric N-deposition, land-use and change, elevation, NDVI, and stream characteristics (temperature and DOC trends). We calculate trends using yearly and seasonal statistics across the last half-century of data acquired by the USGS and

aggregate station trends using station and Hydrological Unit Code (HUC) scales across the CONUS. Statistics include trends in-stream concentrations (*Cn*), temperatures (*T*), discharge rates and volumes (*Qs*), bulk surface water mass exports (*Ex*), and bulk surface water area normalized mass exports or yields (*Ys*). We use the HUC scales as the watershed aggregating units.

2.0 Materials and Methods

We analyzed in-stream C and N concentrations and discharge from USGS National Water Information System (NWIS) stations across the U.S. of six different nitrogen parameters (Supplementary Table A1), one carbon parameter, and temperature (USGS, 2016, 2018) (https://waterdata.usgs.gov/nwis). This big-data approach requires automated analysis to retrieve U.S. Geological streamflow, and concentration data from the long-term monitoring network NWIS using available USGS Web services (Read et al., 2017). We calculated a time-series of total mass exports past a stream station *Ex(t)* (kg/year) using the discharge *Qs(t)* and concentration *Cn(t)* time series by integrating from day 1 of each water year to day 365 for annual time series, and every 3 months for seasonal exports (Equation 1). The mass export is the multiplication of discharge *Qs(t)* (m^3/day) and concentration *Cn(t)* (mg/L converted to kg/m^3) and summed for all daily time steps (dt). Yields were calculated by dividing the total mass export *Ex(t)* (Kg/year or Mg/year) by the drainage area (DA, km^2 or hectare) contributing to watershed yield at that particular station (Kg/km^2/year or Mg/km^2/year) (Equation 2). We converted all values to Kg/hectare, which is the unit associated with the atmospheric deposition time-series.

(1) Export=*Ex(t)*= $\sum_{day\ 1}^{day\ 365} Qs(t)Cn(t)dt$

(2) Yield=$Ys(T)=\frac{\sum_{day\ 1}^{day\ 365} Qs(t)Cn(t)dt}{DA} = \frac{Export}{DA}$

Initial NWIS station selection was based on the criteria that a station was 'maintained' over time and not sampled just once. If a station had *any* available data for *Cn* and *Qs* defined as at least 20 observations of *any* measurements, the station was selected for the next step (see Supplementary Figures A1-A7 for data downloading methods and for station text files). We then subset stations with the criteria that available *Cn* data span across a minimum of 15 years, and contained at least 50 measurements of that *particular* parameter with associated daily *Qs* data. We required stations to have both *Qs* and *Cn* data available (see Supplementary Information A for methods and station files for each NWIS parameter). Since not all NWIS parameters are available at all stations, we used a different set of stations for each parameter. All NWIS data is retrievable through the R packages EGRET and dataRetrieval (Hirsch & De Cicco, 2015). Exports and Yields were calculated at the yearly and seasonal time-scale with daily *Qs*-*Cn* values requiring 365 data points for yearly calculations, and 90 for seasonal calculations. When *Cn* was not available for a particular day, we used a gap-filling approach described below (section 2.1).

The final selection criteria considers the completeness of the station's data across the different hydrologic unit code (HUC) 2-8 scales, and their distribution across elevation categories (Table 1). Each hydrologic unit is identified by a unique HUC consisting of two to eight digits based on the four levels of classification in the hydrologic unit system. As defined by the U.S. Geological Survey, HUC 2-8 scales divide the U.S. into successively smaller hydrologic units which are classified into four levels: regions, sub-regions, accounting units, and cataloging units represented in more common terminology as basin to sub-watershed scales (Seaber et al.,

1987). HUC2 scales represent the largest hydrological region (basin-scales) while HUC8 scales are nested within HUC2 scales and represent cataloging units often referred to as sub-catchments. HUC2 scales represent the largest basin unit within the U.S that contains nested smaller watersheds (Supplementary Table A2 and Supplementary Figure A1). There are 22 distinct HUC2 basins within the U.S that are the largest representative basins (Supplementary Table A2).

Table 1: Information about the number of stations across elevation categories for each NWIS parameter, the range of time water quality data were collected, and the statistics of watershed completeness (i.e. the percentage of watersheds that the stations are found in relative to the total number of watersheds in a given HUC).

			Elevation Categories (m)					Watershed Completeness			
Parameter ID	Short Name	Number of Stations	0-100	100-1000	1000-3000	3000-5000	Time-Series Range	HUC2 (n=22)	HUC4 (n=280)	HUC6 (n=440)	HUC8 (n=2200)
00630	TIN	4988	228	500	896	301	1901-2019*	100.0%	76.1%	78.6%	58.3%
00631	DIN	5666	223	509	937	419	1901-2019	100.0%	77.9%	80.2%	63.2%
00600	TN	6046	260	548	986	378	1901-2019	100.0%	76.4%	80.0%	62.0%
00602	TDN	2650	164	320	492	203	1959-2019	100.0%	75.4%	77.5%	44.4%
00608	DAA	4790	213	443	921	361	1901-2019	100.0%	75.0%	77.0%	58.6%
00610	TAA	5366	238	511	882	297	1901-2019	100.0%	76.1%	78.6%	57.3%
00681	DOC	2520	156	272	443	160	1959-2019	100.0%	76.1%	77.3%	44.2%
00010	Temp	1906	101	175	456	202	1951-2019	95.5%	66.4%	62.3%	36.6%

Descriptions from: https://www.waterqualitydata.us/public_srsnames/

*NWIS ID 09364500 for ANIMAS RIVER AT FARMINGTON, NM is the station with the longest time series. First collected sample was in September 1900 and no collected occurred thereafter until 1971 representing a 70 year gap.

2.1 Gap-filling Datasets

To overcome the problem of sparse concentration and daily discharge data, discharge *Qs(t)* and concentration *Cn(t)* time-series statistics are used to gap-fill the *Cn* time-series using the USGS Weighted Regressions based on Trends, Discharge, and Seasonality (WRTDS) method (Hirsch et al., 2010; Hirsch & De Cicco, 2015; Sinha & Michalak, 2016; Van Meter & Basu, 2017). Additionally, the averaging method (Kothawala et al., 2011; Lovett et al., 2000; Quilbé et al., 2006), and last-observation carried forward (LOCF) method (Moritz et al., 2015) were implemented for comparison to the WRTDS method, the detailed analysis and results of which are found in the Supplementary Information B-Additional Results. Gap-filling methods are necessary for the *Cn(t)* time-series because Equation 1 cannot be calculated for yearly or seasonal exports if *Cn* is not available at each daily time-step. An advantage of WRTDS is the prediction of *Cn* based on *Qs*-*Cn* statistical relationships to obtain hind-cast *Cn* estimates when *Qs* is available. The main drawback of WRTDS is that the hind-casting of *Cn* based on historical *Qs* is often difficult to predict when dry years follow wet years (Pellerin et al., 2014). The R package EGRET offers two predictions of *Cn*: the mean *Cn* based on measured *Qs* and the statistical *Qs*-*Cn* relationship, and the flow normalized *Cn* (*FNC*) which is a normalized value calculated based on the probability density function of *Qs* during that given day assuming that the distribution of discharge is stationary (see EGRET user manual for additional information (Hirsch & De Cicco, 2015)). The *FNC* removes the random variability in *Cn* driven by the random variability in *Qs*. EGRET also offers two predictions of export *Ex*: the *Ex* based on the mean *Cn* and measured *Qs*, and the flow normalized *Ex* (*FNE*) which is a normalized export value calculation based on the *FNC* prediction given the probability density function of *Qs*.

2.2 Trend Detection and Statistical Significance

We analyzed concentration time-series *Cn(t),* flow normalized concentration time-series *FNC(t),* export time-series *Ex(t),* flow normalized export time series *FNE(t),* yield time series *Y(t),* flow normalized yield time series *FNY(t),* and discharge time-series *Qs(t).* We calculated trends for each nitrogen (N) and carbon (C) parameter using two techniques: 1) linear models to extract the slope (β) representing the trend, and 2) Mann-Kendall tests to extract the slope (β_{MK}) representing the trend (Forbes et al., 2019; Helsel & Hirsch, 2002). We analyzed a suite of statistics using the R statistical software for each time series including yearly and seasonal minimum, maximum, and mean values and trends (R Core Team, 2014). Linear models and Mann-Kendall trend tests were only constructed for stations that had >15 years of data available after gap-filling with WRTDS. The predictions and calculations for concentration time-series *Cn(t)* are shown (Equation 3) with concentration (*Cn*) mg/L, slope (β) mg/L/year, time (t) year, and intercept (I) mg/L.

(3) Linear model $Cn(t) = \beta t + I$

Statistical significance of trend tests and persistence of trends were obtained from 1) the significance p-value for the linear slope β at the $p<0.05$ value, 2) the significance p-value for the Mann-Kendall trend parameter β_{MK} (Helsel & Hirsch, 2002) at the $p<0.05$ value, and 3) by calculating the persistence of trends using the Hurst Persistence analysis technique (Dwivedi & Mohanty, 2016; Hurst, 1951) using Hs=0.6 as the persistence cutoff value. We looked at statistical significance of trends using the three methods outlined above to provide robustness to the interpretation of trends (Renwick et al., 2018; Wasserstein & Lazar, 2016).

2.3 Net Atmospheric Deposition, Elevation, Land Cover, and Normalized Differenced Vegetation Index

We directly compared trends in six environmental variables of interest—atmospheric wet and dry N-deposition, land-use/land-use change, stream conditions (temperature and DOC), elevation, drainage area, and Normalized Differenced Vegetation Index (NDVI)—to trends in surface water quality exports and yields. We analyzed the total wet and dry deposition (TDEP, Kg/hectare) of all nitrogen species including NO_3^- and NH_4^+ at the yearly time scale across CONUS from a composite TDEP product available as a smoothed, yearly (once per year) gap-filled CONUS product for years 2000-2018 (NADP, 2018; Schwede & Lear, 2014). The TDEP wet and dry product is a composite product that utilizes the wet deposition product from the National Atmospheric Deposition Program (NADP) including the wet-deposition concentration and loading of NH_4^+, NO_3^-, PRISM precipitation deposition data at yearly time-scales across the U.S., and dry deposition from EPA CASTNET data (EPA CASTNET, 2019; NADP, 2018; Schwede & Lear, 2014). The composite TDEP produce is available as a smoothed, yearly (once per year) gap-filled CONUS product for years 2000-2018 at 4km x 4km pixel sizes. From the total TDEP deposition and the total stream losses (stream yields $Y(t)$) per area, we calculated the watershed retention capacity by subtracting the yearly watershed yield $Y(t)$ as losses (Kg/hectare) from the yearly TDEP depositional inputs (Kg/hectare) (Equation 4) (Lovett et al., 2000). Though we do not directly analyze biogeochemical mechanisms and confounding factors within our study, we acknowledge that a critical insight from all the prior work is that biogeochemical cycling within the watershed is potentially more important to long-term stream exports than atmospheric N-deposition alone (Lovett et al., 2000; Lucas et al., 2016). Internal biogeochemical cycling terms for vegetation sinks (V), soil sinks (S), and gaseous loss sinks (G) (Figure 1) are

biogeochemical terms not accounted for in the retention equation and represent the unknown internal source/sink terms.

(4) Retention Capacity= Ret % = $\frac{Inputs-Losses}{Inputs} * 100 = \frac{TDEP-Yields}{TDEP} * 100$

NDVI, which was obtained from the NASA MODIS satellite, represents broad scale measurements of vegetation productivity, and biomass density, and is important as a controlling factor on nitrogen availability and uptake from deposition in forests. MODIS data are available in a smoothed, gap-filled, monthly CONUS data product for years 2000-2015 with 250m x 250m pixel sizes (Spruce et al., 2016). Land cover (LC) and land cover change (LCC) data were obtained from the Multi-Resolution Land Characteristics (MRLC) consortium National Land Cover Database (NLCD) and represents the total land cover type across the CONUS for years 2001, 2008, and 2016, as well as the total change between 2001 and 2016 and have 30 x 30 m pixel sizes (MRLC NLCD, 2020; Yang et al., 2018). We did not calculated trends from LC, rather we used LC and LCC as a grouping variable. Elevations were obtained from a CONUS scale digital elevation model (DEM) 1km x 1km pixel sizes (Maurer, 2016; Maurer et al., 2004). Associated elevation categories (Elev groups) are defined as such: Low Elevation < 30m, Medium Elevation (30-300m), Moderate Elevation (300-1500m), High Elevation > 1500m. Elevations categories represent arbitrary cutoffs. Seasonal trends were calculated by aggregating three month increments into each season: spring (March-April-May), summer (June-July-August), fall (September-October-November), and winter (December-January-February). It is unknown what the error of these products are.

We calculated yearly and seasonal trends for all variables, and compared the trends accordingly across different TDEP, NDVI, LC, and Elev groups. TDEP-NDVI grouping categories in Figure 2 were used to represent distinct regions with unique watershed stages of N-saturation. We used the Kruskall-Wallis test for statistical significance between groups of data such as *Ex* trends across Elev categories, or *Cn* trends across all increasing or decreasing NDVI groups. All variable names, trend short-hand notation, and trend units used in this study are shown in Table 2.

Table 2: Table of variables used, units, symbols to represent the variable and the relevant trend (slope) units.

Variable	Units	Symbol	Time-Series	Slope (β or βMK)	Slope Units
Concentration	mg/L	*C*	*C(t)*	ΔC	mg/L/year
Discharge	m^3/s	*Q*	*Q(t)*	ΔQ	m^3/year
Export	Kg/day	*E*	*E(t)*	ΔE	Kg/year or Mg/year
Yield	$Kg/km^2/day$	*Y*	*Y(t)*	ΔY	Kg/ha/year or Mg/ha/year
Flow Normalized Concentration	mg/L	*FNC*	*FNC(t)*		mg/L/year
Flow Normalized Export	Kg/d	*FNE*	*FNE(t)*		Kg/year or Mg/year
Flow Normalized Yield	$Kg/km^2/day$	*FNY*	*FNY(t)*		Kg/ha/year or Mg/ka/year
Normalized Differenced Vegetation Index	unitless	*NDVI*	*NDVI(t)*	$\Delta NDVI$	"-"/year
Total Wet+Dry Nitrogen Deposition	Kg/ha	*TDEP*	*TDEP(t)*	$\Delta TDEP$	kg/ha/year
Elevation	m	*ELEV*			

2.4 Watershed Aggregation

Once station-based statistics, models, and trends were constructed, the slope values and the statistics were aggregated to the different hydrologic unit code (HUC) 2-8 scales. When aggregating trends from the station to the larger HUC2-HUC8 scales, we used two approaches:

Simple averaging: We used simple averaging of trends across all stations to get the aggregated HUC2-HUC8 trends. We used this approach to map average trends in ΔE, ΔC, ΔY and ΔQ. For example, all station slopes (β) for concentration were averaged for each HUC8 region to provide an average slope for that HUC8 region. When averaging the *Q* data for each WQP, we averaged using only the stations where the particular WQP values were available. When aggregating the *Q* data to the basin or watershed scales, we used all available *Q* data across all WQP for that basin. We evaluated the significance of these trends by counting the number of stations within each watershed that were statistically significant at $p<0.05$. Additionally, we averaged only statistically significant station trends across groups: TDEP-NDVI groups, elevation groups, and land cover.

Area-Weighted averaging: Area-weighted averaging is a method of aggregating values by applying weight to the values based on another variable. We calculated area-weighted averages by weighting the trend values using contributing drainage areas such that exports from larger contributing areas provide more weight to the average than exports from smaller contributing areas. For example, when calculating the area-weighted average concentration for a HUC8 region, downstream concentrations have more weight applied in the averaging step than upstream concentrations.

Statistical significance of trends was obtained from the previously described approaches: linear correlation (Equation 2), Mann-Kendall tests, Hurst Exponent Persistence for each *C(t), Q(t), Y(t),* and *E(t)* trend for each water parameter, and for each environmental variable of

interest (NDVI, TDEP, LC, Elev, Temp). Statistical significance was assessed at the $p<0.05$ value for linear model derived slopes (β), and for Mann-Kendall slopes (β_{MK}), and at the $Hs>0.6$ level for Hurst Persistence significance. To aggregate the statistical significance from the station scale to the HUC 2-8 scale, we used a station thresholding approach to identify how many watersheds contain more than 50% of stations with statistically significant and directionally similar trends in ΔE and ΔC, or ΔE and ΔQ. We compared trends in station ΔE, ΔC, ΔY, and ΔQ and counted the number of stations showing statistically significant ($p<0.05$) and directionally similar trends (positive or negative) in these variables for every HUC2-HUC8 watershed. We also used this approach to quantify the number of watersheds within four categories: similar ΔE-ΔC trends, opposite ΔE-ΔC trends, similar ΔE-ΔQ trends, and opposite ΔE-ΔQ trends to evaluate the role of concentration and discharge on long-term trends. We counted how many stations, and what percentage of stations within each HUC2-HUC8 watershed fall in the four TDEP-NDVI grouping categories. Because this CONUS 'big-data' approach requires a significant amount of computational capabilities, all data processing and analysis was performed on the LBNL NERSC supercomputer CORI cluster. We used over 30000 core hours requiring over 500Gb of memory on the Cori 'Big-Memory' node and analyzed over 1Tb of data.

3.0 Results

Our results section is structured as follows: we first present results of the trend analysis for TDEP, NDVI, and in-stream parameters for DIN, DOC, and Temp related to our first research question (section 3.1, 3.2, and 3.3). We then examine how watershed exports and watershed retention relate to the conceptualized TDEP-NDVI groups presented in Figure 2 to address our second research question (section 3.4). Finally, we provide results examining potential

491 controlling factors on watershed retention including land use and elevation, and describe the
492 modalities of watershed retention hysteresis and one-way transition patterns (section 3.5 and
493 3.6).
494
495 **3.1 TDEP-NDVI Grouping Classification**

496 Considerable spatial variability in TDEP and NDVI trends is found across the CONUS
497 (Figure 3). General patterns across a few HUC2 scales are highlighted. In HUC2 basin #10
498 (Missouri Basin), patterns of increasing NDVI and increasing TDEP (Group a) reflect the
499 majority of HUC8 scale watersheds within the Missouri. Across the South Atlantic-Gulf Basin
500 (HUC2 #03), increasing trends in NDVI are associated with decreases in TDEP (Group c). In the
501 Ohio Basin (HUC2 #05), decreasing patterns of NDVI are observed with decreasing patterns in
502 TDEP (Group d). Across the Pacific Northwest Basin (HUC2 #17), spatial variability in N-
503 saturation groups are found with regions showing difference in TDEP and NDVI. Many HUC8
504 regions within the Pacific Northwest fall into Group b, representing increases in TDEP and
505 declines in NDVI. Across the CONUS, 50% of HUC8 watersheds fall into Group a, 20% in
506 Group b, 20% in Group c, and 10% in Group d. We use the TDEP-NDVI groupings throughout
507 the rest of the paper to facilitate interpretation of watershed N-losses and N-retention trends.
508 TDEP-NDVI groups and their conceptualized role on in-stream trends are provided in Figure 2.

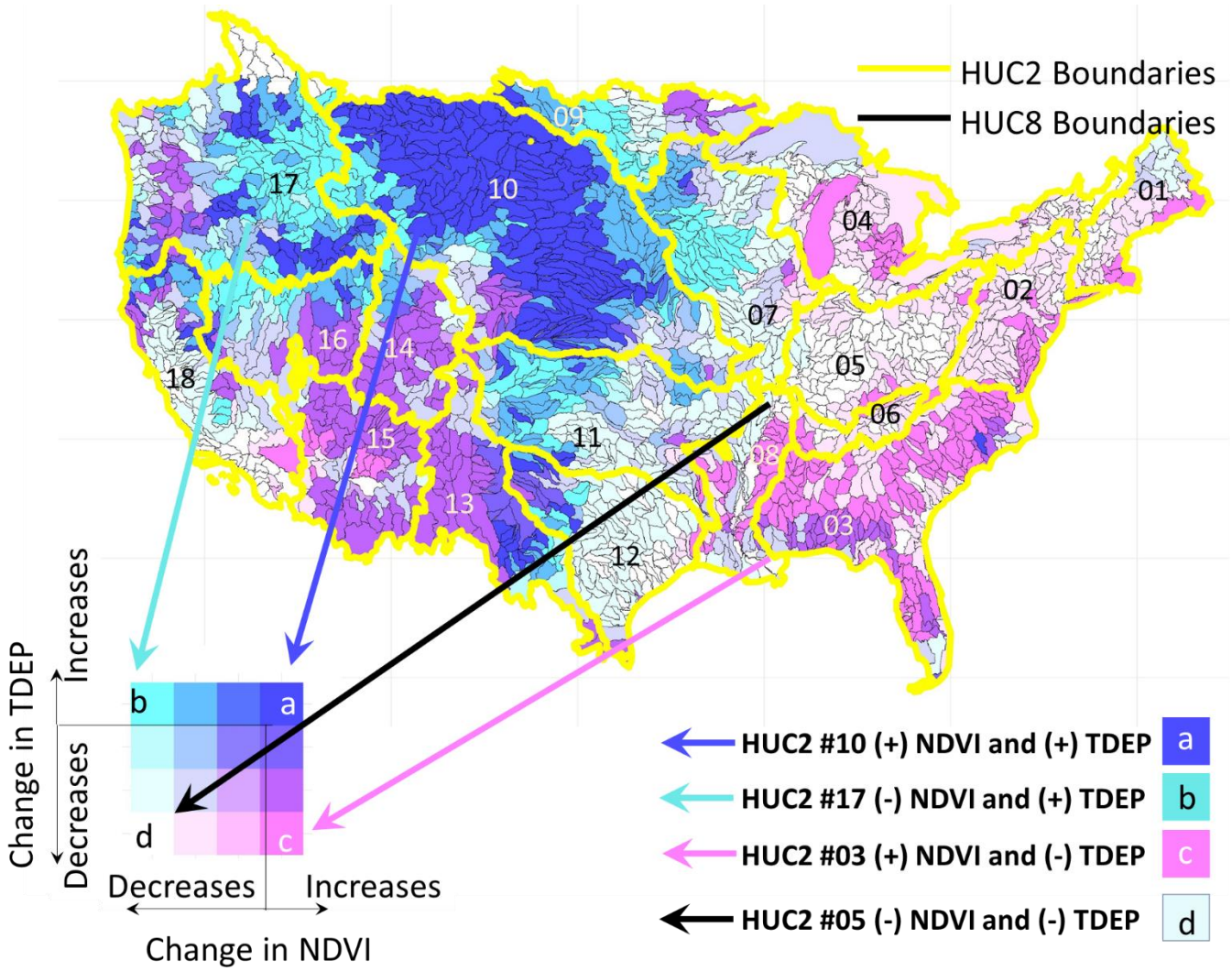

Figure 3: Groupings and directionality of vegetation and deposition change based on trends in TDEP (2000-2018) and NDVI (2000-2015). Groupings include: : Group a) regions with increasing NDVI and increasing TDEP, Group b) regions with decreasing NDVI and increasing TDEP, Group c) regions with increasing NDVI and decreasing TDEP, and Group d) regions with decreasing NDVI and decreasing TDEP. HUC2 boundaries are shown by the yellow line with their corresponding HUC2 basin numbers. Groups a-d and their colors are used consistently throughout the rest of this paper and refer to the same groups illustrated in Figure 2 and defined in Section 1.0.

3.2 Concentration Trends across US Basins

CONUS-wide DIN concentration trends across HUC4 watersheds shows wide-variability (Figure 4). All means are calculated from stations with statistical significance only. Statistical significance was evaluated with the linear trend parameter, the Mann-Kendall trend parameter, and the Hurst persistence parameter. Across the CONUS, 36.5% of stations show statistically significant declining concentrations of DIN (-0.005 ± 0.004 mg/L/year), while 38.1% of stations show statistically significant increasing concentrations of DIN (+0.0082 ± 0.0092 mg/L/year). It is common for water quality datasets to have such large standard deviations because of interannual variability (i.e. (Strauss et al., 2004)). We highlight six HUC2 watersheds, four from Figure 3 (HUC2 #03, HUC2 #05, HUC2 #10, HUC2 #17) which represent the Groups a-d, and two additional HUC2 watersheds to contrast results (HUC2 #14, and HUC2 #12). Tables of DIN concentration statistics for these six watersheds are provided in Supplementary Table B1. Of these six basins, we find the largest DIN concentrations across the Texas Gulf Basin (HUC #12) (1.88 ± 3.04 mg/L), with average increasing rates of change (β = 0.007 ± 0.053, β_{MK} = 0.01 ± 0.068 mg/L/year). These rates contrast basins such as the Upper Colorado HUC #14 (0.33 ± 0.57 mg/L), 49.1% of stations show statistically significant trends and show a declining rate of change (β = -0.007 ± 0.027, β_{MK} = -0.003 ± 0.026 mg/L/year). The Upper Colorado has the lowest concentrations of DIN among the six basins. In the Ohio Basin (HUC2# 05), average DIN concentrations are 1.78 ± 3.38 mg/L. The Ohio Basin shows the largest average rates of decline with a majority of stations (nSLP/nS >50%) showing statistically significant downward trends (β = -0.03 ± 0.14 mg/L/year, β_{MK} = -0.04 ± 0.18 mg/L/year). The number of stations showing

541 significance of Mann-Kendall trend parameters generally agrees with the significance of the
542 linear parameter (nSLP ≈ nSMKP). Trend statistical significance calculated with the Hurst
543 Persistence parameter shows a larger fraction of stations have persistent trends than the linear or
544 Man-Kendall parameters (see for example HUC#10, nSH = 251). Tables of statistics for all other
545 HUC2 watersheds, statistical significance, linear, and Mann-Kendall trends are also provided in
546 Supplementary Table B1.
547

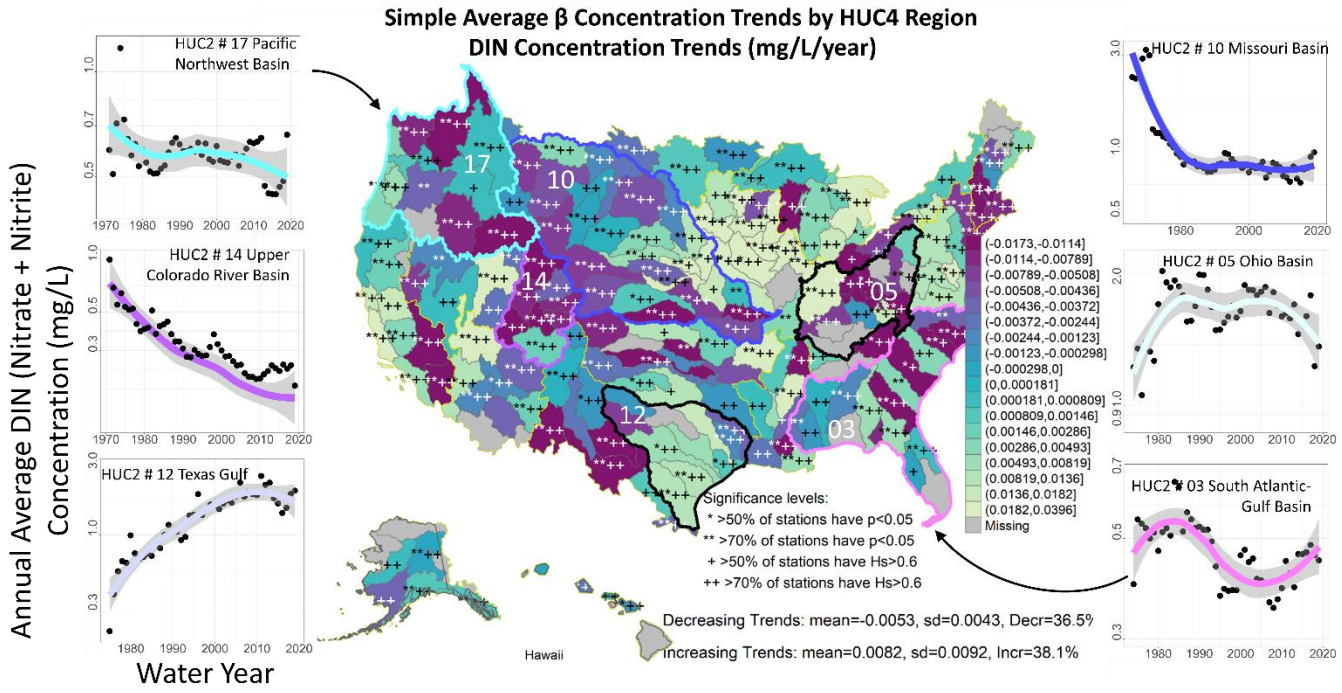

548

549 Figure 4: Trends in DIN concentrations *C(t)* from 1970-2020 for the CONUS and select HUC2
550 basins #17, 14, 12, 10, 05, and 03 are shown with the same colors corresponding to the groupings
551 in Figure 3. Trends are shown from the average gap-filling method and β trends calculated for
552 each station and aggregated up using Simple Averaging. Trends statistics are provided in
553 Supplementary Table B1. Average annual DIN concentrations over time are shown for the
554 selected six HUC2 basins. Significant levels are indicated by the following symbols: * >50% of

555 stations have p<0.05, **>70% of stations have p<0.05, + >50% of stations have Hs>0.6, and ++
556 > 70% of stations have Hs>0.6.
557

558 Similarly, across the CONUS we find increasing and decreasing trends in DOC
559 concentrations for the different HUC2 and HUC4 basins from 1970-2020 (Figure 5), however
560 major gaps in DOC coverage occur across the CONUS. On average, 57.9% of HUC4 watersheds
561 show statistically significant decreasing concentrations (-0.067 ± 0.049 mg/L/year), while 14.5%
562 of HUC4 watersheds show statistically significant increasing concentrations (0.022 ± 0.027
563 mg/L/year). We find the largest DOC concentrations across the South-Atlantic Gulf Basin (HUC
564 #03) (13.36 ± 13.79 mg/L), with the lowest rates of DOC change (β = 0.037 ± 0.33, β_{MK} = 0.035
565 ± 0.34 mg/L/year). In the Missouri Basin HUC #10, average concentrations (5.78 ± 4.65 mg/L)
566 are coupled with the largest rates of DOC concentration change (β = -0.080 ± 0.13, β_{MK} = -0.081
567 ± 0.17 mg/L/year). Tables of statistics for all other HUC2 watersheds, statistical significance,
568 linear, and Mann-Kendall trends are also provided in Supplementary Table B2. We also provide
569 trend maps for all other water parameters in Supplementary Figure B1-B2. Temperature maps
570 with the same selected six HUC2 basins (Supplementary Figure B3) and temperature statistics
571 are also provided (Supplementary Table B3).

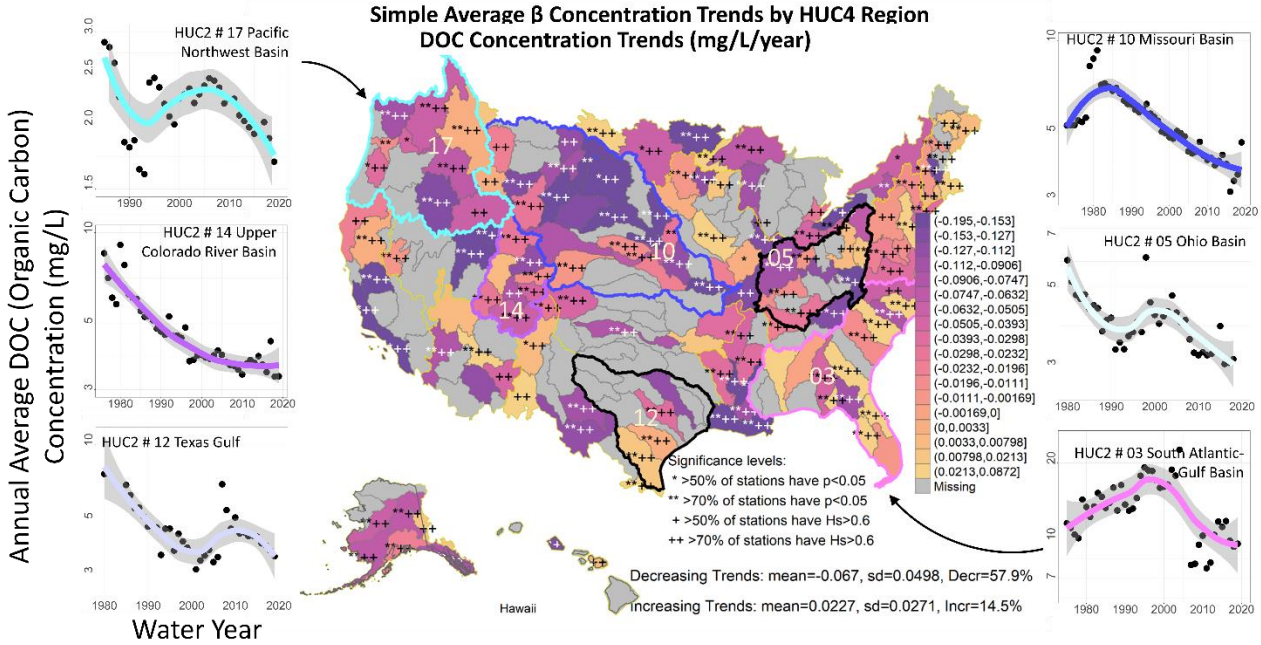

572

573 Figure 5: Trends in DOC concentrations *C(t)* from 1970-2020 for the CONUS and select HUC2
574 basins #17, 14, 12, 10, 05, and 03 are shown with the same colors corresponding to the groupings
575 in Figure 3. Trends are shown from the average gap-filling method and β trends calculated for
576 each station and aggregated up using Simple Averaging. Trends statistics are provided in
577 Supplementary Table B2. Average annual DOC concentrations over time are shown for the
578 selected six HUC2 basins. Significant levels are indicated by the following symbols: * >50% of
579 stations have p<0.05, **>70% of stations have p<0.05, + >50% of stations have Hs>0.6, and ++
580 > 70% of stations have Hs>0.6.

581

582 **3.3 The Role of Trends in Discharge on Trends in Exports across US Basins**

583 Calculations of DIN exports (watershed losses) represent the combined effect of discharge
584 and concentration in a basin (Equation 1) and are directly used in the calculation of watershed N-
585 retention (Equation 4). *Trends* in DIN exports (linear β parameter for *Ex(t)* Mg/year) across all

586 U.S. stations, aggregated to U.S. HUC4 watersheds show patterns of spatial variability in the
587 direction (increasing or decreasing) and statistical significance similar to concentration trends
588 (Figure 4, Supplementary Figure B4). We found 34.8% of all stations (nS = 1136) across
589 CONUS showed statistically significant decreasing trends in DIN exports (β = -3.2 ± 4.2
590 Mg/year, outliers > 99th percentile and < 1st percentile removed) (Supplementary Figure B4A).
591 Another 22.3% of CONUS stations show statistically significant increasing DIN export trends (β
592 = 8.4 ± 13.9 Mg/year, outliers > 99th percentile and < 1st percentile removed). Aggregating all of
593 the station export data *Ex(t)*) to all the HUC2 levels shows similar variability in magnitude and
594 distribution of DIN export change across the CONUS (Supplementary Table B4, Supplementary
595 Figure B5). Tables and maps of discharge, exports and their statistics are provided in
596 Supplementary Figures B6-B9 and Tables B4-B7).

597 Trends in watershed exports are not only important for determining watershed retention
598 metrics, but also for characterizing future changes in N and C deliveries to coastlines. The
599 magnitude and direction of DIN export *trends* relative to the magnitude of yearly exports ranges
600 between -16 – 24% per decade (all HUC2 decadal changes are provided in Supplementary Table
601 B4). HUC #14, for example, shows a decline in DIN exports of -16.9% over the next decade,
602 which is the largest declining rate relative to the other HUC2 basins, albeit quite low in
603 magnitude (-66.9 Mg over the next decade). By comparison, HUC #17 also shows a decline in
604 DIN exports of -4.6% over the next decade but a much larger magnitude (-127.7 Mg over the
605 next decade). We aggregated these annual estimates of DIN and DOC trends to calculate total
606 coastal exports from the land to the ocean from coastal abutting basins (specifically HUC2 #01,
607 02, 03, 08, 12, 13, 15, 17, 18, 19, 20). Across the coastal basins directly exporting N and C to the
608 ocean, we found annual average coastal N and C exports are declining. Total dissolved inorganic

609 nitrogen exports (sum of filtered nitrate, nitrite, ammonia, ammonium) have declined by
610 approximately 60% over the past two decades (1970-2000: 9.4 Tg-N/year, 2000-2020: 3.72 Tg-
611 N/year), and organic carbon exports have declined by approximately 80% over the past two
612 decades (1970-2000:19.5 Tg-C/year, 2000-2020: 3.72 Tg-N/year).

613 While discharge is always the most significant contributor to yearly export magnitudes on an
614 inter-annual basis, we found no conclusive evidence that decadal *trends* in discharge are the most
615 significant contributor to decadal *trends* in exports (Figure 6). We found statistically significant
616 discharge trends at < 10% of all CONUS stations (Supplementary Figure B9, Table B5).
617 Correlations between trends in *Cn(t)* and *Ex(t)* were statistically significant at the $p<0.001$ level
618 (Figure 6 a,b) while correlations between trends in *Qs(t)* and *Ex(t)* were statistically significant at
619 the $p=0.04$ level (Figure 6 c,d). We observed that while changes (*trends*) in DIN and DOC
620 exports are driven by *both* concentration and discharge (Supplementary Figure B10, B11),
621 changes in exports were more often associated with changes in concentration rather than
622 discharge (Supplementary Table B8). When correlating decadal *trends* in discharge and
623 concentration to *trends* in exports for all water parameters, we found directionally similar and
624 statistically significant trends in *Cn(t)* and *Ex(t)* across more than 25% of stations. Conversely,
625 we found directionally similar and statistically significant trends in *Qs(t)* and *Ex(t)* at <3% of
626 stations (Supplementary Table B8).
627
628

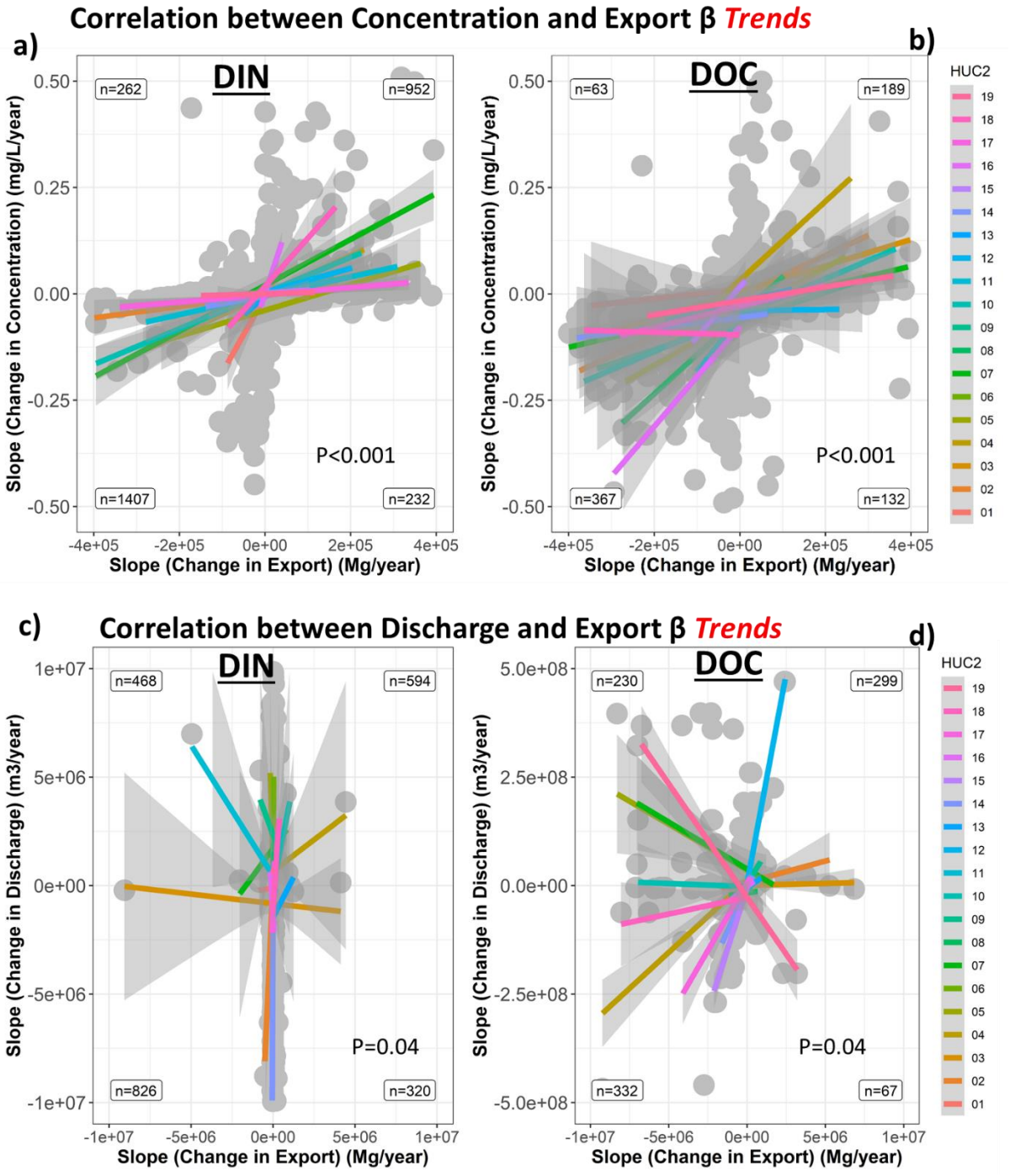

Figure 6: Correlations between trends in concentration and exports (a, b) and correlations between trends in discharge and exports (c,d) for DIN and DOC and each HUC2 basin shown by the various colors. Total statistical significance for the trends is provided in each figure. Each quadrant shows the number of stations (n) that fall within each quadrant.

634

635

636 **3.4 Trends in Watershed Exports for NDVI-TDEP Groups**

637 We examined trends in watershed exports across the NDVI-TDEP Groups to examine the
638 degree to which CONUS scale atmospheric deposition patterns, vegetation trends, and stream
639 trends can be potential indicators of watershed N-retention conditions conceptualized in our
640 watershed hysteresis model (Figure 2). Trends in *E(t)* (Mg/year) for DIN and DOC obtained
641 from all stations and aggregated by NDVI-TDEP groups from Figure 3 show distinct trends that
642 support our conceptual model (Figure 7). DIN shows similar modes of variability across the
643 TDEP-NDVI groups for both exports and yields: greater declines in exports (mean β = -9.97 ±
644 148.5 Mg/year) and yields (mean β = -0.001 ± 0.04 Kg/hectare/year) in Group a, with steady
645 increases across the TDEP-NDVI groups towards increasing exports (mean β = 59.08 ± 148.8
646 Mg/year) and yields (mean β = 0.13 ± 0.56 Kg/hectare/year) in Group d. DIN export trends in
647 Group a (declining trends) are associated with in-stream concentration declines (-0.0016
648 mg/L/year ±), and DIN export trends in Group d (increasing trends) are associated with in-
649 stream DIN concentration increases (+0.0052 mg/L/year ±) (colors in Figure 7 indicate
650 concentration trends). DIN export trends show statistically significant differences between
651 Groups a-d (K.W. p=0.0015). DOC export trends are statistically significant between groups
652 (K.W. p=0.0055) and show an interesting pattern of reversal from Group a to d: declines in
653 exports are found for Group a and Group d (Group a mean β = -444 ± 574 Mg/year, Group d
654 mean β = -854 ± 2253 Mg/year), but a greater proportion of increasing trends are found in Group
655 b (mean β = 115 ± 114 Mg/year). DOC concentrations are declining for all groups except for
656 Group c (0.0011 mg/L/year). Trends in *E(t)* (Mg/year) and *Y(t)* (Kg/hectare/year) by NDVI-

TDEP group for all water parameters are provided in Supplementary Figure B12. Seasonally aggregated barplots are provided in Supplementary Figure B13.

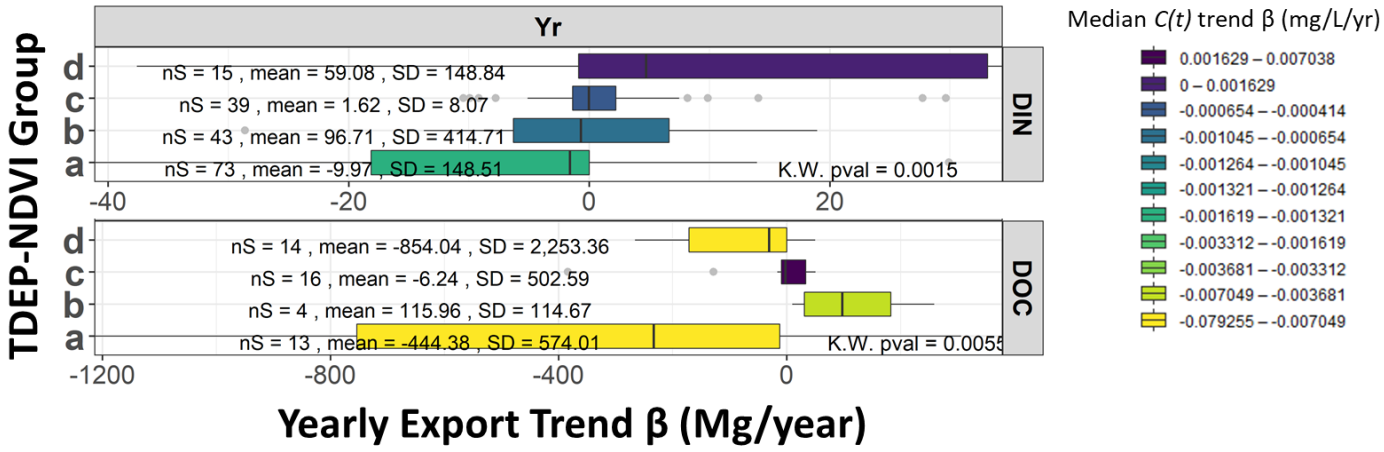

Figure 7: Box plots of the export and yield data separated by WQP and NDVI-TDEP groups. Boxplots show the median as the middle line, upper (75%) and lower (25%) quartiles as ends of the box, and upper and lower fences representing 1.5 times the inter-quartile range. If there are outliers more or less than 1.5 times the upper or lower quartiles, respectively, they are shown with grey dots. All trend results are colored based on the associated median trends in *C(T)*. Colors represent median values of concentration change for that box (mg/L/year). The number of statistically significant stations (nS), the mean and standard deviation are shown next to each box. All statistics were calculated using only stations with statistically significant trends ($p<0.05$). As a reminder of the TDEP-NDVI grouping representations, Groups a (+TDEP, +NDVI), Group b (+TDEP, -NDVI), Group C (-TDEP, +NDVI), and Group d (-TDEP, -NDVI).

3.5 Retention across U.S. Basins

674 Watershed retention (Equation 4, TDEP inputs minus watershed exports) of atmospheric
675 TDEP across all U.S. HUC4 basins reveals wide variability in retention patterns (Figure 8) when
676 compared by region or NDVI-TDEP group. The lowest retention values across the CONUS
677 occur in the Midwest region (HUC2 #07 mean retention = 35%) (Figure 8 a,b, Supplementary
678 Table B8). By contrast, most regions across the U.S. have high watershed N-retention (>90%)
679 and sustain high retention values before 2007 (Figure 8a) and after 2007 (Figure 8b) (2007 is an
680 arbitrary year to evaluate temporal trends by comparing means). Retention calculations across
681 CONUS also reveal differences when assessed between NDVI-TDEP groups (Figure 8c). Most
682 HUC8 watersheds classified as Group a, retain close to 100% of incoming atmospheric TDEP
683 (median = 98.6%, mean = 93.3%, s.d. = 17.6%) (Figure 8c). Watersheds classified within Group
684 d retain about one-half to two-thirds of incoming TDEP (median = 77.8%, mean = 61.8%, s.d. =
685 42.1%). As expected based on the proposed conceptual model (Figure 2), once watersheds
686 become N-saturated (occurs around Group b), retention of incoming N-deposition decreases and
687 more is lost directly to watershed exports leading to lower retention values (Groups c and d).
688 Retention statistics calculated for each HUC2 basin are provided in Supplementary Table B8.
689

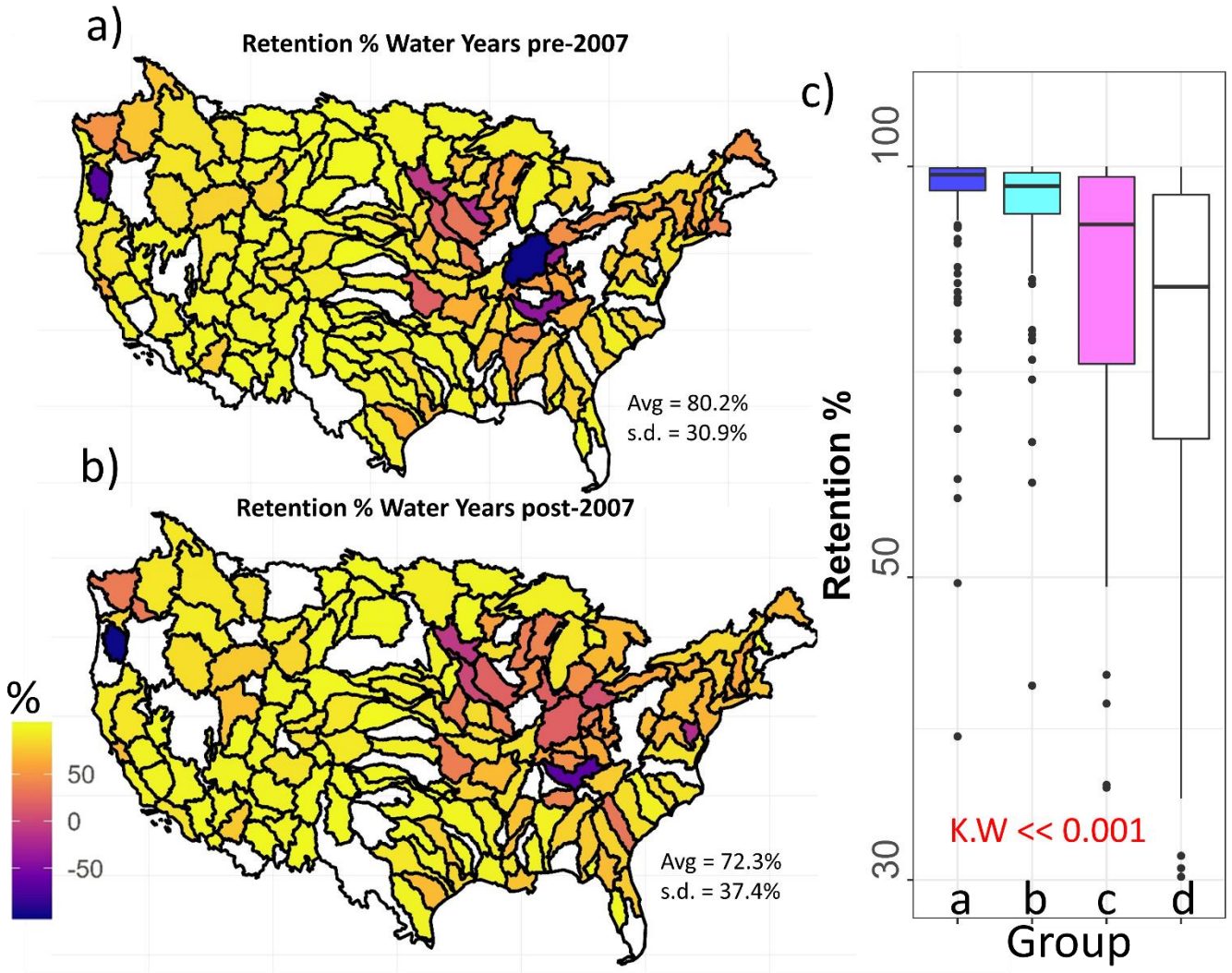

Figure 8: a) Spatial distributions and averages of retention (% Retention) are shown for HUC4 watersheds across the CONUS before 2007, b) Spatial distributions and averages of retention are shown for HUC4 watersheds across the CONUS after 2007, c) Box plots of retention are shown for the different TDEP-NDVI groups and show statistically significant differences (K.W. << 0.001). As a reminder of the TDEP-NDVI grouping representations, Groups a (+TDEP, +NDVI), Group b (+TDEP, -NDVI), Group C (-TDEP, +NDVI), and Group d (-TDEP, -NDVI).

699 Across HUC8 watersheds, retention is found to vary as a function of land-use
700 characteristics and NDVI-TDEP groups (Figure 9). Retention varies across the different NDVI-
701 TDEP groups in a similar fashion to that shown in Figure 8 with larger retention values on
702 average in Group a (92.5% ± 19.5 %) and lower retention values in Group d (61.1% ± 40.6 %).
703 For each land-cover class, K.W values for differences between NDVI-TDEP groupings are
704 statistically significant. Forest land cover shows highly variable retention across the NDVI-
705 TDEP groups with the lowest retention found in Group b (-13.0% ± 36.9 %). The negative value
706 for Group b indicates an additional source of N is present (outputs > atmospheric inputs). Planted
707 land-cover types, which include cultivated crops and pasture/hay also show a general decline in
708 retention from Group a (91.9% ± 20.5%) to Group d (51.5% ± 43.5%), but with much larger
709 distribution of values in Group b. Wetland land cover types show close to 100% retention for
710 NDVI-TDEP Groups a and b, and then trend downward for Groups c and d. Maximum land-
711 cover types and changes by HUC2 basin are provided in the Supplementary Figure B14.
712 Maximum land-cover types and changes by NDVI-TDEP group and year are provided in the
713 Supplementary Figure B15.
714
715

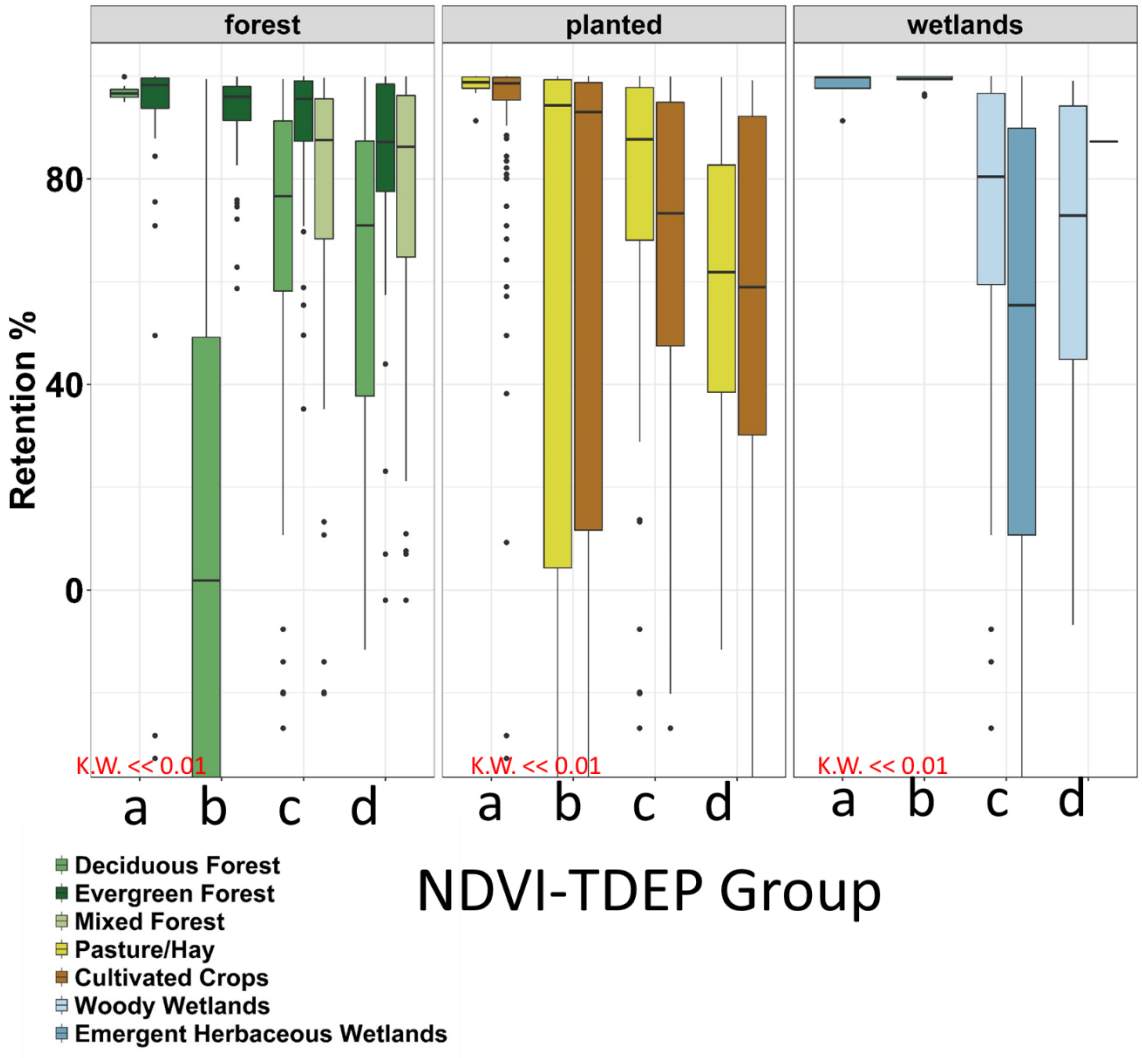

Figure 9: N-retention across NDVI-TDEP groups and further refined by different land cover class and types (forest, planted, and wetlands). Colors represent the different land-cover groups within each broad land-cover class.

Comparing the total percent of variance in watershed N-retention explained by the four groups of interest (land cover, NDVI-TDEP group, Elevation, and stream factors which include stream temperature/DOC concentrations), our results indicate that land cover may not be the primary controlling factor on watershed N-retention (Table 3). The total percent of variance in

watershed N-retention explained by land cover type ranges between 0.15-30.8 % (average 9.97%) which is the third largest factor among the four explanatory groups. NDVI-TDEP groups primarily explain, on average a greater percent of the variance in watershed N-retention (range 4.03-45.14%, average 16.13%). Stream factors which include the combined temperature and DOC concentration dataset explain the second largest percent of variance in watershed N-retention (range 0.04-36.85%, average 13.23%). Regionally, land cover is a second order control within the Lower Mississippi River basin (HUC 08, explains 30.8% of variability in N-retention) despite land cover being of lesser importance in the five other HUC2 basins that contribute directly to the Lower Mississippi (Arkansas White Red HUC 11, Missouri HUC 10, Upper Mississippi HUC 07, Ohio HUC 05, Tennessee HUC 06). The Mid-Atlantic Basin (HUC #02) is the only basin where land cover is identified as a primary co-variate to watershed N-retention. The inclusion of the land-cover change dataset explained such a significantly low percentage of variability (<0.0001%) that we do not show those results here and we excluded that variable from the analysis.

Table 3: Percent of variability in watershed N-retention explained by the four different variables of interest for each HUC 2 basin. The percent of variability explained by each variable was calculated using the ANOVA statistical analysis and statistical significance of each variable is indicated in parentheses.

Percent of Variability In Watershed N-Retention Explained

HUC	Maximum Land Cover Class	NDVI-TDEP Group	Elevation	Stream Factors (Temperature and DOC)
01	0.25(0.144)	11.69(0)	0.5(0.038)	19.82(0)
02	20.16(0)	6.51(0)	0.28(0.012)	11.49(0)
03	2.98(0)	15.91(0)	0.07(0.372)	6.88(0)
04	7.45(0)	12.52(0)	0.68(0.001)	11.39(0)
05	9.95(0)	12.27(0)	1.1(0.025)	11.19(0)
06	3.48(0.008)	17.12(0)	4.52(0.003)	13.12(0)
07	19.29(0)	34.83(0)	0.09(0.14)	5.47(0)
08	30.8(0)	45.14(0)	0(0.862)	12.53(0)
09	8.08(0)	35.4(0)	5.79(0)	6.08(0)
10	9.19(0)	11.09(0)	4.03(0)	6.89(0)
11	11.94(0)	16.95(0)	0.82(0)	3.55(0)
12	14.57(0)	4.03(0)	0.21(0.095)	21.73(0)
13	0.16(0.398)	4.77(0)	2.11(0.002)	12.78(0)
14	10.07(0)	6.74(0)	1.6(0)	32.64(0)
15	5.92(0)	17.56(0)	29.39(0)	4.57(0)
16	1.72(0.002)	19.13(0)	1.61(0.003)	24.89(0)
17	0.87(0)	16.8(0)	0.45(0)	36.88(0)
18	22.75(0)	6.91(0)	0.98(0)	31.74(0)
Average	9.97%	16.40%	3.01%	15.17%
	1	9	1	7

* p-values are shown in parentheses

3.6 Modalities of Watershed Retention and Hysteresis

TDEP and NDVI are important controlling factors on watershed N-retention patterns, and our results demonstrate evidence for watershed N-hysteresis across the range of deposition environments (Figure 10a). Watersheds with high retention capacity (where >90% of N is retained, red dots) show a trend toward increasing NDVI with TDEP—watersheds with high

755 retention capacity have the potential to store excess N in biomass and likely become N-saturated
756 as TDEP increases (TDEP range 3-10 Kg/hectare/year, NDVI range 0.2-0.6, Figure 10a).
757 Watersheds with low retention capacity (<20% of N is retained, blue dots) are N-saturated or
758 undergoing recovery from N-saturation and show a different relationship with NDVI and TDEP
759 than the high-retention capacity group (Figure 10a). Low-retention watersheds undergoing
760 reversal from N-saturation show that NDVI remains high for all values of TDEP and appears to
761 decline quite significantly once TDEP is < 3 Kg/hectare/year. Our results show that the
762 relationship between NDVI and TDEP differs depending on how saturated the watershed is and
763 the state of NDVI and TDEP. Lower initial values of NDVI are associated with the increasing
764 NDVI group while larger initial values of NDVI are associated with the decreasing NDVI groups
765 (Figure 10c). Similarly with TDEP, lower values are within the increasing TDEP category, and
766 larger values are in the decreasing TDEP category (Figure 10b). Watersheds with a high N-
767 retention capacity are generally associated with regions of increasing TDEP and NDVI patterns,
768 while watersheds with a low N-retention capacity are generally associated with regions of
769 decreasing NDVI and TDEP patterns. As the first line of evidence supporting N-hysteresis in
770 watersheds, these generalizable patterns suggest that eventual recovery from excess N-deposition
771 may include a lagged response and a legacy of compromised forest health.
772
773

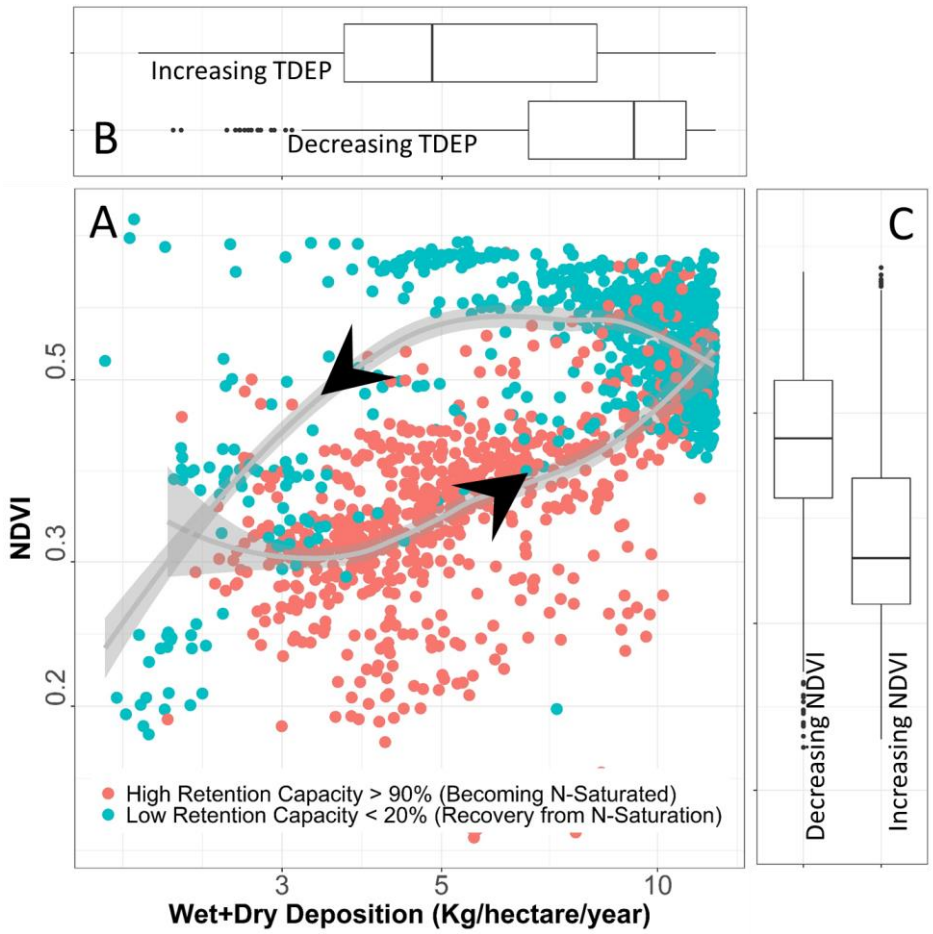

774

775 Figure 10: a) Scatterplot of NDVI and TDEP colored by high (red dots) and low (blue dots)
776 watershed N-retention capacity. High retention capacity watersheds are those that retain most
777 atmospheric deposition and have very low losses in stream exports. Low retention capacity
778 watersheds are those that lose most atmospheric deposition to stream losses. B) Boxplot
779 distribution TDEP values (associated with x-axis) grouped by trends in TDEP. C) Boxplot
780 distribution of NDVI values (associated with y-axis) grouped by trends in NDVI.

781

782

783 Hysteresis and one-way transition patterns of watershed N-retention and loss for a few
784 select individual HUC8 watersheds reveal varying modalities of N-retention and recovery are

possible (Figure 11). The highlighted watersheds with permanent changes (i.e. one-way transition to a new steady-state) are represented by maximum land cover types of Evergreen Forest-72.34% (permanent increase in retention, Figure 11a), and Deciduous Forest-38.08% (permanent decrease in retention, Figure 11b). A transition from Evergreen Forest to Grassland is observed (86.16% coverage in 2001 to 72.34% in 2016) and associated with a one-way increase in retention and decreases in losses (Figure 11a). One-way declines in retention and increases in losses are found in HUC8 #02080103 (Rapidan-Upper Rappahannock. Virginia) with a dominant land cover type classified as Deciduous Forest (Figure 11b). The percent of the dominant land cover class (Deciduous Forest) does not change much over the 2000-2016 time period. Some land cover change does occur (-1.1% conversion of Pasture to Cultivated Crops, Grassland) (Figure 11b). The watersheds with one-way increase and loss patterns (Figure 11a, b) are notable because they potentially represent watersheds that have transitioned beyond an equilibrium state in response to N deposition or other changes.

Clockwise and counterclockwise hysteresis patterns representing the systems recovery to initial conditions also emerge (Figures 11c, d, e, f, g, h). In some cases, the watershed moves to a new state represented by changes in both retention and loss (Figure 11c, e), or the watershed returns to the original state represented by values of retention and loss that are at or near the initial state (Figure 11f, g). This might be interpreted as having an unperturbed biogeochemical cycling capacity such that it can sustain significant deviations from the original state and still return to the original state. Watersheds with Retention ≈ 0% are rare (n=14 out of 2119 HUC8 watersheds) and represent watersheds with close to equal inputs (TDEP) and outputs (losses or Yields), 3 of which occur in the Upper Mississippi (HUC2 #07). These watersheds either have a significantly perturbed N-cycle due to some other anthropogenic factor and only represent a

steady state condition such that inputs = outputs. However, they could also represent a subset of watersheds lacking significant biogeochemical capacity. Watersheds with outputs greater than inputs are similarly rare, representing <5% of watersheds (n=103 out of 2119 HUC8 watersheds), 29 of which are in the Upper Mississippi (HUC2 #07). Watersheds representing near pristine conditions, with retention close to 100%, represent ~12% of HUC8 watersheds (n=251 out of 2119 HUC8 watersheds), 65 of which are in the Missouri Basin (HUC2 #10, 58% Grassland/Herbaceous, Supplementary Figure B13). The rare, perturbed, and pristine HUC8 watersheds are listed in Supplementary Table B9. While we highlight individual watersheds here, we also recognize many watersheds do not have clear patterns and require much greater interrogation into underlying processes.

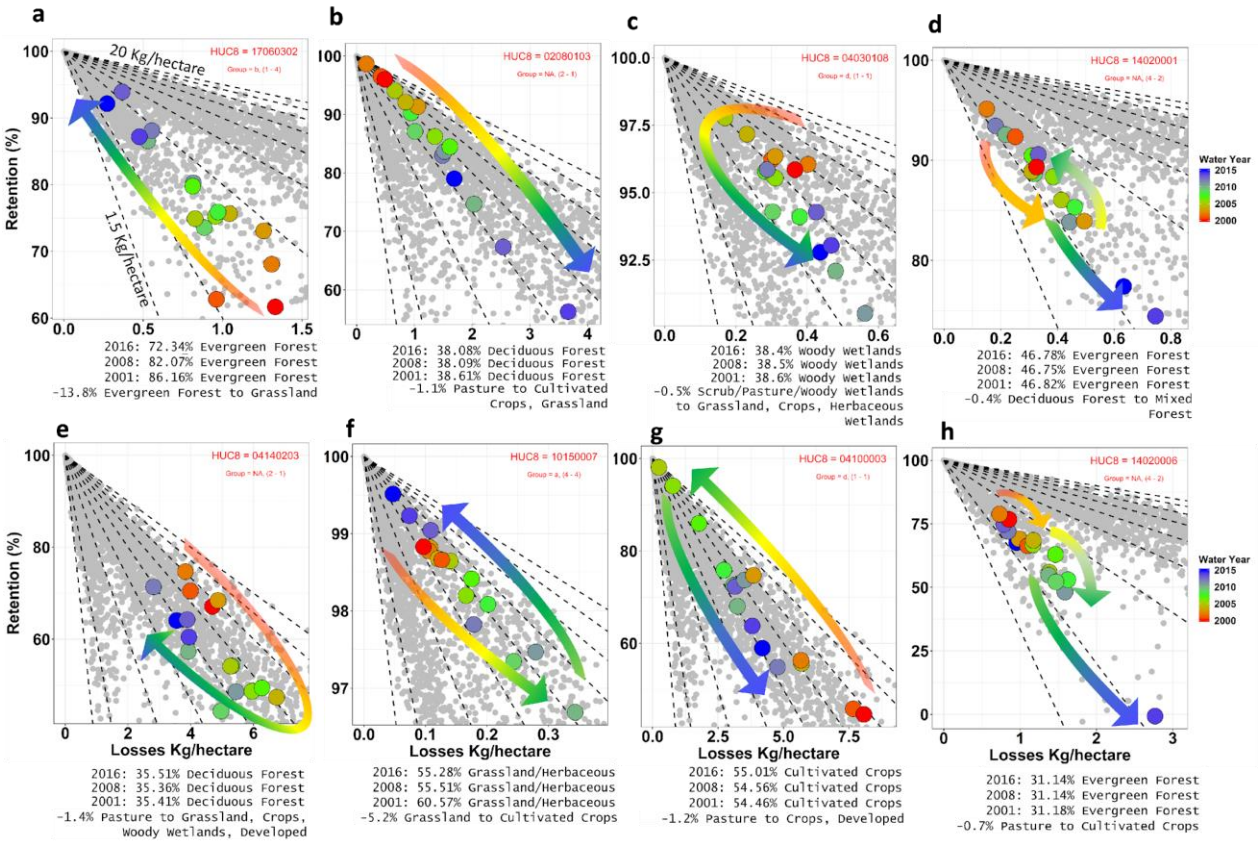

Figure 11: Scatter plots and hysteresis curves of HUC8 watershed retention (%) (y-axis) and loss (x-axis) (Kg/hectare) in individual HUC8 watersheds. Dashed lines represent lines of equal TDEP (Kg/hectare) ranging from 1.5-20 Kg/hectare. Colors represent the water year and are increasing from the year 2000 (red) to 2015 (blue). Arrows are shown that follow the time series of colors (red to blue representing the year 2000-2015) and show either the one-way transition or the hysteresis pattern. If the arrow curves in a circular pattern, hysteresis is identified, but if the arrow is uni-directional, then this is a one-way transition. Percentages below each figure represent the land cover type with the maximum percentage coverage for each year.

4.0 Discussion

In this study, we examine the degree to which CONUS scale atmospheric deposition patterns, vegetation trends, and stream trends can be potential indicators of watershed N-saturation, retention, and recovery conditions, and how watershed N retention and losses vary over space and time. We provide evidence for the hysteresis behavior of N-saturation and retention in watersheds using a time series of CONUS stream losses relative to CONUS atmospheric deposition inputs and NDVI. We highlight watershed N-retention patterns across groups of atmospheric deposition and vegetation productivity/biomass to advance understanding of stream trends as indicators of watershed N conditions, and reveal patterns of watershed N-hysteresis (recovery) or transition patterns.

4.1 Stream Trends Reveal Watershed N-Hysteresis Patterns

Several lines of evidence here support the hysteretic conceptual model of watershed N retention and recovery (Figure 2). First, we found that atmospheric deposition (TDEP) and vegetation (NDVI) groups that display combinations of strong positive or negative trends over time, are associated with patterns of stream exports that uniquely indicate the stage of watershed N-saturation (Figure 8) and reveal modalities of watershed N-retention hysteresis or one-way transition patterns (Figure 11). In particular, we found regions with increasing TDEP and increasing NDVI *trends* (Group a, Figure 2) have close to 100% N-retention (Figure 9c), become increasingly N-saturated over time (Figure 11) and are associated with the strongest declines in DIN and DOC exports (Figure 8). Conversely, we find a tendency towards increasing trends in DIN exports and much lower retention in regions associated with TDEP-NDVI Group d where watersheds retain about 50 - 66 % of incoming TDEP. Second, trends in DIN export that coincide with trends in DOC export also help to identify the stage of watershed N-retention and direction of change based on our updated N-hysteresis conceptual model. Since DOC movement to streams is a function of the size of the watershed C pool, in-stream DOC concentration measurements combined with DIN measurements can provide an important proxy of catchment responses to N deposition and input. Third, by examining how watershed N-retention has changed over time, we found that watersheds display a variety of types of recovery (hysteresis) or non-recovery (one-way) patterns. Our findings agree with the hypotheses presented by Lovett et al., (2018) that areas at late successional stages (i.e., those in Group d) should show much less retention than their aggrading counterparts (Group a). We hope that our work can provide value to future interpretation of in-stream trends and provides a new conceptual model such that in-

stream DIN and DOC *trend* signatures can be used as indicators of watershed N-retention status (Gilliam et al., 2019; Goodale et al., 2003, 2005).

4.2 Drivers of N-retention, and hysteresis patterns across the CONUS

We found that regional trends in-stream exports (*Ex*) were more often correlated to trends in concentration (*Cn)* rather than trends in discharge (*Qs)*. This reveals that the dominant contributing factor to *changes in magnitude and direction of trends* of *Ex* are more often determined by changes in concentrations than flow. This emphasizes the significant role of 1) watershed biogeochemical cycling and processes (soil and biomass immobilization, in-stream biogeochemistry etc.) across the critical zone as major factors shaping in-stream concentrations, and 2) the significant role of environmental physical/chemical conditions (TDEP-NDVI group) that facilitate uptake and retention of N. While the lack of influence of *Qs* has been noted previously (Goodale et al., 2003; Lucas et al., 2016), drivers of trends in *Ex* can be hydrological, biogeochemical, or an external factor (e.g. agriculture), whereas, the observed trends in *Qs* and *Cn* can be indicators of changing watershed N functionality through vegetative, soil, or in-stream biogeochemical pathways. For example, the insignificant role of discharge trends on determining overall trends in exports and concentrations may be more directly related to the stage of watershed N-saturation, evapotranspiration control on depth of hydrological flow paths, and newly acquired access of flowpaths to stores of older N and C not readily assessable prior to transitions in TDEP-NDVI stage (Barnes et al., 2018). Indeed, residence times of water versus N particles within a watershed are different and can vary from years to decades depending on inter-annual or anthropogenic conditions (Sinha & Michalak, 2016). Much recent work in watershed acid-rain mitigation experiments suggests that the ‘flashiness’ of N export during storm events

might be an important indicator of watershed N-retention and saturation status because of shifts in N sourcing form more distal and shallow parts of the watershed (Marinos et al., 2018). Despite the lack of significant trends in discharge observed in our study, more work will be needed assessing how hydrological conditions coincide with broad scale physical/chemical conditions as described by TDEP-NDVI patterns that impact flow paths and access to different stores and cycling of C and N in landscapes.

4.3 In-stream processes

The second-largest factor explaining variability in watershed N-retention across HUC2 basins was in-stream temperature and DOC concentration trends (Table 3). This result provides evidence that in-stream measurements can potentially can be indicators of watershed functionality by interpreting stream signals as aggregated measurements and proxies to those upstream watershed conditions. The consequence of changing N and C transfer from the terrestrial to the aquatic setting is the mediation of in-stream assimilation and hyporheic redox conditions at downstream locations. In-stream and hyporheic biogeochemistry provides an important control on stream exports once nutrients reach the stream through in-stream assimilation and hyporheic denitrification (Arora et al., 2016; Cejudo et al., 2018; Hood et al., 2017). Declining stream N exports due to increased watershed N retention may lead to steady or increasing DO concentrations in downstream ecosystems and transition to oligotrophic conditions (Craine et al., 2018; Groffman et al., 2018). Changes in aquatic primary production can occur in response to changing nitrogen inputs (from atmospheric deposition and watershed delivery) and seasonality (Bernhardt & Likens, 2004), which can shift denitrification rates and patterns through direct and indirect coupling to labile carbon exudates and oxygen conditions

910 (Heffernan & Cohen, 2010). Conversely, in low elevation or more anthropogenic sites, rising
911 temperatures and increases in N transfer to streams could coincide with declining DO
912 concentrations and more eutrophic conditions, greater in-stream N-assimilation, particularly in
913 N-limited water bodies (Beaulieu et al., 2011; Bernhardt et al., 2002; Halliday et al., 2013), and
914 greater hyporheic denitrification (Bernhardt et al., 2005; Duncan et al., 2013, 2015; Maavara et
915 al., 2019; Mulholland et al., 2009; Newcomer et al., 2018; Seitzinger et al., 2006). The influence
916 of stream factors on watershed N-retention before land use/cover was a surprising aspect of this
917 analysis. Because stream and hyporheic residence times are so short, this conclusion indicates
918 that instream processes are probably substantially more influential than expected, in terms of the
919 overall magnitude of control on stream exports.
920

921 **4.4 Confounding factors**

922 We found that watershed retention is quite high (>70% for most watersheds across the U.S.)
923 relative to atmospheric inputs, a finding similar to other published work (Lovett et al., 2000). It is
924 important to note that any external contributions to in-stream DIN concentrations and exports not
925 accounted for in this study (i.e. agriculture) would be additional input terms in the retention
926 equation. These retention estimates are likely an underestimate of watershed N retention because
927 there is uncertainty related to source terms from the lack of information on anthropogenic inputs
928 across these watersheds. We do not account for agriculture input to our retention equation which
929 means that our retention estimates are potentially significant *underestimates* of retention. Since
930 exports and TDEP are the measured values in the retention equation, we estimate that in the most
931 intensively managed agricultural regions, we are underestimating retention by 50-100% (25
932 Kg/hectare/year)(Van Meter et al., 2016).

933 Surprisingly, while we found that land cover, and in particular land cover change data
934 was the least significant factor controlling N export and retention, we acknowledge that
935 consideration of potential drivers of some stream N trends depends somewhat on to what extent
936 these watersheds receive urban or agricultural N inputs and how these have changed. For
937 example, we found more spatially consistent decreasing trends in stream DAA exports and
938 concentrations across the CONUS which might be more likely to reflect change in fertilizer or
939 sewage N inputs. The lack of significance between watershed N-retention and land cover/change
940 data may also point to legacy N in watersheds. Given the history of N deposition and
941 anthropogenic application on ecosystems, there is great potential for lagged responses and
942 geochemical stationarity in stream N and C because of significant water and N residence times
943 (Basu et al., 2010).
944 Other confounding factors not included in this analysis are the occurrence of extreme event
945 hydrological conditions (Argerich et al., 2013), shifts in the abundance of dominant vegetation
946 within classes (Argerich et al., 2013; Bernal et al., 2012; Compton et al., 2003; Rhoades et al.,
947 2017; Sudduth et al., 2013; Van Breemen et al., 2002), changes in vegetation aboveground
948 biomass and plant populations in response to varying alpine snow-hydrological conditions
949 (Hubbard et al., 2018), and changes in reforested areas could explain an overall decline in NO_3^-
950 export within the stream (Bernal et al., 2012). In other studies, declines of in-stream N have been
951 found in regions with greatest soil N accumulation and during the growing season indicating a
952 biologically mediated trend in DIN and no correlation with hydrology (Lucas et al., 2016).
953 Similar to Goodale et al., (2005) we find patterns in DOC concentrations across these watersheds
954 that support the hypothesized mechanism that enhanced ecosystem productivity increases fluxes
955 of labile carbon from the soil to the stream, enhancing denitrification leading to declining stream

N trends. Finally, the importance of climatic control on soil N processes cannot be emphasized enough. Longer growing seasons, with warmer climates and elevated CO_2 have been shown to change nitrogen and carbon availability terrestrial soils (Terrer et al., 2018). Plant uptake and N mineralization both respond to soil moisture, temperature, and climatic patterns such that any changes in the rate or timing of these processes can tilt watersheds beyond their ability to retain or release nitrogen in a hysteretic manner.

5.0 Conclusion

In many watersheds across the CONUS, stream exports of DIN have been declining and show enduring legacies from N-deposition and acid rain. To examine large scale controls on stream DIN and DOC concentration and export trends, we developed an updated hysteresis conceptual model of watershed N-retention and examined how two main controlling landscape-scale controls (TDEP and NDVI) can be used to group patterns of stream loss and watershed retention. Our hysteresis conceptual model provides a novel framework for which to assess watershed N-retention and recovery patters as indicated by stream DIN and DOC trends. Our conceptual model is validated with a quantitative analysis of stream data (DIN, DOC, temperature), NDVI, land cover, and TDEP trends that reveal specific patterns of stream loss that are associated with modalities of watershed hysteresis (recovery) or one-way transition (new steady state) patterns. For the first time, we show that watershed retention of N can display unique hysteresis patterns, and that these patterns can be explained by the wealth of detailed mechanistic studies available for watersheds at different stages of response to changing N-deposition. In its present form, our conceptual model can offer a valuable new insight into

decade's worth of stream water data collection, and highlight the value of stream water measurements as critical indicators of upstream watershed functionality.

6.0 Acknowledgements

This material is based upon work supported as part of the Watershed Function Scientific Focus Area funded by the U.S. Department of Energy, Office of Science, Office of Biological and Environmental Research under Award Number DE-AC02-05CH11231. We acknowledge the Total Deposition (TDEP) Science Committee of the National Atmospheric Deposition Program (NADP) for their role in making the TDEP data and maps available. All analyzed data used for this study can be found here: All original data can be obtained from the various sources listed here. MODIS data are available at: http://dx.doi.org/10.3334/ORNLDAAC/1299. NLCD land cover and land cover change data are available at: https://doi.org/10.5066/P937PN4Z. Elevation raster data are available at: https://www.hydroshare.org/resource/c18cef883695498c81acf9c4260d1e53/. Stream water N, C, and temperature data are available at: https://waterdata.usgs.gov/nwis. NADP composite TDEP CONUS Product is available at: http://nadp.slh.wisc.edu/committees/tdep/tdepmaps/. All watershed boundary shapefiles are available from the USGS Watershed Boundary Dataset (WBD) of the National Geospatial Program (https://usgs.gov/core-science-systems/ngp/national-hydrography). All gap-filled NWIS datasets that are merged with the CONUS scale NDVI, TDEP, Land Cover, and Elevation products that are produced within this study will be made freely available on ESS-DIVE (https://ess-dive.lbl.gov/) for free-public access upon acceptance of this article. All station files for each water parameter will also be included in the data publication on ESS-DIVE.

7.0 Author Contributions

MN, HW, NB, SH contributed to experimental design. MN, DD, KW, and HW contributed to data collection and analysis. MN, DD, EW contributed to code design. MN, NB, TM, BA, EW, KW, CS, SH contributed to data interpretation. MN prepared the manuscript with contributions from all authors.

8.0 References

Aber, J. D., McDowell, W., Nadelhoffer, K., Magill, A., Berntson, G., Kamakea, M., et al. (1998). Nitrogen Saturation in Temperate Forest Ecosystems. *BioScience*, *48*(11), 921–934. https://doi.org/10.2307/1313296

Aber, J. D., Goodale, C. L., Ollinger, S. V., Smith, M.-L., Magill, A. H., Martin, M. E., et al. (2003). Is Nitrogen Deposition Altering the Nitrogen Status of Northeastern Forests? *BioScience*, *53*(4), 375. https://doi.org/10.1641/0006-3568(2003)053[0375:INDATN]2.0.CO;2

Argerich, A., Johnson, S. L., Sebestyen, S. D., Rhoades, C. C., Greathouse, E., Knoepp, J. D., et al. (2013). Trends in stream nitrogen concentrations for forested reference catchments across the USA. *Environmental Research Letters*, *8*(1), 014039. https://doi.org/10.1088/1748-9326/8/1/014039

Arora, B., Spycher, N. F., Steefel, C. I., Molins, S., Bill, M., Conrad, M. E., et al. (2016). Influence of hydrological, biogeochemical and temperature transients on subsurface carbon fluxes in a flood plain environment. *Biogeochemistry*, *127*(2–3), 367–396. https://doi.org/10.1007/s10533-016-0186-8

1025 Ballard, T. C., Sinha, E., & Michalak, A. M. (2019). Long-Term Changes in Precipitation and
1026 Temperature Have Already Impacted Nitrogen Loading. *Environmental Science &*
1027 *Technology*, *53*(9), 5080–5090. https://doi.org/10.1021/acs.est.8b06898
1028 Barnes, R. T., Butman, D. E., Wilson, H. F., & Raymond, P. A. (2018). Riverine Export of Aged
1029 Carbon Driven by Flow Path Depth and Residence Time. *Environmental Science &*
1030 *Technology*, *52*(3), 1028–1035. https://doi.org/10.1021/acs.est.7b04717
1031 Beaulieu, J. J., Tank, J. L., Hamilton, S. K., Wollheim, W. M., Hall, R. O., Mulholland, P. J., et
1032 al. (2011). Nitrous oxide emission from denitrification in stream and river networks.
1033 *Proceedings of the National Academy of Sciences*, *108*(1), 214–219.
1034 https://doi.org/10.1073/pnas.1011464108
1035 Bellmore, R. A., Compton, J. E., Brooks, J. R., Fox, E. W., Hill, R. A., Sobota, D. J., et al.
1036 (2018). Nitrogen inputs drive nitrogen concentrations in U.S. streams and rivers during
1037 summer low flow conditions. *Science of The Total Environment*, *639*, 1349–1359.
1038 https://doi.org/10.1016/j.scitotenv.2018.05.008
1039 Bernal, S., Hedin, L. O., Likens, G. E., Gerber, S., & Buso, D. C. (2012). Complex response of
1040 the forest nitrogen cycle to climate change. *Proceedings of the National Academy of*
1041 *Sciences*, *109*(9), 3406–3411. https://doi.org/10.1073/pnas.1121448109
1042 Bernhardt, E. S., & Likens, G. E. (2004). Controls on periphyton biomass in heterotrophic
1043 streams. *Freshwater Biology*, *49*(1), 14–27. https://doi.org/10.1046/j.1365-
1044 2426.2003.01161.x
1045 Bernhardt, E. S., Hall, Jr., R. O., & Likens, G. E. (2002). Whole-system Estimates of
1046 Nitrification and Nitrate Uptake in Streams of the Hubbard Brook Experimental Forest.
1047 *Ecosystems*, *5*(5), 419–430. https://doi.org/10.1007/s10021-002-0179-4

1048 Bernhardt, E. S., Likens, G. E., Hall, R. O., Buso, D. C., Fisher, S. G., Burton, T. M., et al.
1049 (2005). Can't See the Forest for the Stream? In-stream Processing and Terrestrial
1050 Nitrogen Exports. *BioScience*, *55*(3), 219. https://doi.org/10.1641/0006-
1051 3568(2005)055[0219:ACSTFF]2.0.CO;2
1052 Bowden, R. D., Wurzbacher, S. J., Washko, S. E., Wind, L., Rice, A. M., Coble, A. E., et al.
1053 (2019). Long-term Nitrogen Addition Decreases Organic Matter Decomposition and
1054 Increases Forest Soil Carbon. *Soil Science Society of America Journal*, *83*(S1).
1055 https://doi.org/10.2136/sssaj2018.08.0293
1056 Boyer, E. W., Howarth, R. W., Galloway, J. N., Dentener, F. J., Green, P. A., & Vörösmarty, C.
1057 J. (2006). Riverine nitrogen export from the continents to the coasts: RIVERINE
1058 NITROGEN EXPORT. *Global Biogeochemical Cycles*, *20*(1), n/a-n/a.
1059 https://doi.org/10.1029/2005GB002537
1060 Cejudo, E., Hood, J. L., Schiff, S. L., & Aravena, R. O. (2018). Using the δ15N of submerged
1061 biomass for assessing changes in the nitrogen cycling in a river receiving wastewater
1062 treated effluent. *Ecological Indicators*, *95*, 645–653.
1063 https://doi.org/10.1016/j.ecolind.2018.08.013
1064 Compton, J. E., Church, M. R., Larned, S. T., & Hogsett, W. E. (2003). Nitrogen Export from
1065 Forested Watersheds in the Oregon Coast Range: The Role of N 2 -fixing Red Alder.
1066 *Ecosystems*, *6*(8), 773–785. https://doi.org/10.1007/s10021-002-0207-4
1067 Craine, J. M., Elmore, A. J., Wang, L., Aranibar, J., Bauters, M., Boeckx, P., et al. (2018).
1068 Isotopic evidence for oligotrophication of terrestrial ecosystems. *Nature Ecology &*
1069 *Evolution*, *2*(11), 1735–1744. https://doi.org/10.1038/s41559-018-0694-0

1070 Crawford, J. T., Hinckley, E.-L. S., Litaor, M. I., Brahney, J., & Neff, J. C. (2019). Evidence for
1071 accelerated weathering and sulfate export in high alpine environments. *Environmental*
1072 *Research Letters*, *14*(12), 124092. https://doi.org/10.1088/1748-9326/ab5d9c
1073 Cusack, D. F., Silver, W. L., Torn, M. S., Burton, S. D., & Firestone, M. K. (2011). Changes in
1074 microbial community characteristics and soil organic matter with nitrogen additions in
1075 two tropical forests. *Ecology*, *92*(3), 621–632. https://doi.org/10.1890/10-0459.1
1076 Driscoll, C. T., Driscoll, K. M., Roy, K. M., & Mitchell, M. J. (2003). Chemical Response of
1077 Lakes in the Adirondack Region of New York to Declines in Acidic Deposition.
1078 *Environmental Science & Technology*, *37*(10), 2036–2042.
1079 https://doi.org/10.1021/es020924h
1080 Duncan, J. M., Groffman, P. M., & Band, L. E. (2013). Towards closing the watershed nitrogen
1081 budget: Spatial and temporal scaling of denitrification. *Journal of Geophysical Research:*
1082 *Biogeosciences*, *118*(3), 1105–1119. https://doi.org/10.1002/jgrg.20090
1083 Duncan, J. M., Band, L. E., Groffman, P. M., & Bernhardt, E. S. (2015). Mechanisms driving the
1084 seasonality of catchment scale nitrate export: Evidence for riparian ecohydrologic
1085 controls: SEASONALITY OF CATCHMENT NITRATE EXPORT. *Water Resources*
1086 *Research*, *51*(6), 3982–3997. https://doi.org/10.1002/2015WR016937
1087 Dwivedi, D., & Mohanty, B. (2016). Hot Spots and Persistence of Nitrate in Aquifers Across
1088 Scales. *Entropy*, *18*(1), 25. https://doi.org/10.3390/e18010025
1089 EPA CASTNET. (2019). Clean Air Status and Trends Network (CASTNET) EPA CASTNET
1090 Total Wet and Dry Deposition. Retrieved from https://www.epa.gov/castnet

1091 Eshleman, K. N., Sabo, R. D., & Kline, K. M. (2013). Surface Water Quality Is Improving due to
1092 Declining Atmospheric N Deposition. *Environmental Science & Technology*, *47*(21),
1093 12193–12200. https://doi.org/10.1021/es4028748
1094 Evans, C. D., Reynolds, B., Jenkins, A., Helliwell, R. C., Curtis, C. J., Goodale, C. L., et al.
1095 (2006). Evidence that Soil Carbon Pool Determines Susceptibility of Semi-Natural
1096 Ecosystems to Elevated Nitrogen Leaching. *Ecosystems*, *9*(3), 453–462.
1097 https://doi.org/10.1007/s10021-006-0051-z
1098 Forbes, W. L., Mao, J., Ricciuto, D. M., Kao, S., Shi, X., Tavakoly, A. A., et al. (2019).
1099 Streamflow in the Columbia River Basin: Quantifying Changes Over the Period 1951-
1100 2008 and Determining the Drivers of Those Changes. *Water Resources Research*, *55*(8),
1101 6640–6652. https://doi.org/10.1029/2018WR024256
1102 Garayburu-Caruso, V. A., Stegen, J. C., Song, H.-S., Renteria, L., Wells, J., Garcia, W., et al.
1103 (2020). Carbon Limitation Leads to Thermodynamic Regulation of Aerobic Metabolism.
1104 *Environmental Science & Technology Letters*, acs.estlett.0c00258.
1105 https://doi.org/10.1021/acs.estlett.0c00258
1106 Gilliam, F. S., Burns, D. A., Driscoll, C. T., Frey, S. D., Lovett, G. M., & Watmough, S. A.
1107 (2019). Decreased atmospheric nitrogen deposition in eastern North America: Predicted
1108 responses of forest ecosystems. *Environmental Pollution*, *244*, 560–574.
1109 https://doi.org/10.1016/j.envpol.2018.09.135
1110 Goodale, C. L., Aber, J. D., & Vitousek, P. M. (2003). An Unexpected Nitrate Decline in New
1111 Hampshire Streams. *Ecosystems*, *6*(1), 0075–0086. https://doi.org/10.1007/s10021-002-
1112 0219-0

1113 Goodale, C. L., Aber, J. D., Vitousek, P. M., & McDowell, W. H. (2005). Long-term Decreases
1114 in Stream Nitrate: Successional Causes Unlikely; Possible Links to DOC? *Ecosystems*,
1115 *8*(3), 334–337. https://doi.org/10.1007/s10021-003-0162-8
1116 Groffman, P. M., Driscoll, C. T., Durán, J., Campbell, J. L., Christenson, L. M., Fahey, T. J., et
1117 al. (2018). Nitrogen oligotrophication in northern hardwood forests. *Biogeochemistry*,
1118 *141*(3), 523–539. https://doi.org/10.1007/s10533-018-0445-y
1119 Guo, D., Lintern, A., Webb, J. A., Ryu, D., Liu, S., Bende-Michl, U., et al. (2019). Key Factors
1120 Affecting Temporal Variability in Stream Water Quality. *Water Resources Research*,
1121 *55*(1), 112–129. https://doi.org/10.1029/2018WR023370
1122 Hale, R. L., Grimm, N. B., Vörösmarty, C. J., & Fekete, B. (2015). Nitrogen and phosphorus
1123 fluxes from watersheds of the northeast U.S. from 1930 to 2000: Role of anthropogenic
1124 nutrient inputs, infrastructure, and runoff. *Global Biogeochemical Cycles*, *29*(3), 341–
1125 356. https://doi.org/10.1002/2014GB004909
1126 Halliday, S. J., Skeffington, R. A., Wade, A. J., Neal, C., Reynolds, B., Norris, D., & Kirchner, J.
1127 W. (2013). Upland streamwater nitrate dynamics across decadal to sub-daily timescales:
1128 a case study of Plynlimon, Wales. *Biogeosciences*, *10*(12), 8013–8038.
1129 https://doi.org/10.5194/bg-10-8013-2013
1130 Heffernan, J. B., & Cohen, M. J. (2010). Direct and indirect coupling of primary production and
1131 diel nitrate dynamics in a subtropical spring-fed river. *Limnology and Oceanography*,
1132 *55*(2), 677–688. https://doi.org/10.4319/lo.2010.55.2.0677
1133 Helsel, D. R., & Hirsch, R. M. (2002). *Statistical Methods in Water Resources*. U.S. Geological
1134 Survey. Retrieved from http://pubs.usgs.gov/twri/twri4a3/

1135 Hirsch, R. M., & De Cicco, L. (2015). *User guide to Exploration and Graphics for RivEr Trends*
1136 *(EGRET) and dataRetrieval: R packages for hydrologic data (version 2.0, February*
1137 *2015)*. Retrieved from https://dx.doi.org/10.3133/tm4A10
1138 Hirsch, R. M., Moyer, D. L., & Archfield, S. A. (2010). Weighted Regressions on Time,
1139 Discharge, and Season (WRTDS), with an Application to Chesapeake Bay River Inputs.
1140 *JAWRA Journal of the American Water Resources Association*, *46*(5), 857–880.
1141 https://doi.org/10.1111/j.1752-1688.2010.00482.x
1142 Hood, J. M., Benstead, J. P., Cross, W. F., Huryn, A. D., Johnson, P. W., Gíslason, G. M., et al.
1143 (2017). Increased resource use efficiency amplifies positive response of aquatic primary
1144 production to experimental warming. *Global Change Biology*.
1145 https://doi.org/10.1111/gcb.13912
1146 Hubbard, S. S., Williams, K. H., Agarwal, D., Banfield, J., Beller, H., Bouskill, N., et al. (2018).
1147 The East River, Colorado, Watershed: A Mountainous Community Testbed for
1148 Improving Predictive Understanding of Multiscale Hydrological–Biogeochemical
1149 Dynamics. *Vadose Zone Journal*, *17*(1), 0. https://doi.org/10.2136/vzj2018.03.0061
1150 Hungate, B. A., Lund, C. P., Pearson, H. L., & Chapin, Iii, F. S. (1997). Elevated CO2 and
1151 nutrient addition after soil N cycling and N trace gas fluxes with early season wet-up in a
1152 California annual grassland. *Biogeochemistry*, *37*(2), 89–109.
1153 https://doi.org/10.1023/A:1005747123463
1154 Huntington, T. G. (2005). Can Nitrogen Sequestration Explain the Unexpected Nitrate Decline in
1155 New Hampshire Streams? *Ecosystems*, *8*(3), 331–333. https://doi.org/10.1007/s10021-
1156 004-0105-z

1157 Hurst, H. E. (1951). Long-term Storage Capacity of Resevoirs. In *Transactions of the American*
1158 *Society of Civil Engineers* (Vol. 116, pp. 770–799). American Society of Civil Engineers.
1159 Janssens, I. A., Dieleman, W., Luyssaert, S., Subke, J.-A., Reichstein, M., Ceulemans, R., et al.
1160 (2010). Reduction of forest soil respiration in response to nitrogen deposition. *Nature*
1161 *Geoscience*, *3*(5), 315–322. https://doi.org/10.1038/ngeo844
1162 Jensen, A. M., Scanlon, T. M., & Riscassi, A. L. (2017). Emerging investigator series: the effect
1163 of wildfire on streamwater mercury and organic carbon in a forested watershed in the
1164 southeastern United States. *Environmental Science: Processes & Impacts*, *19*(12), 1505–
1165 1517. https://doi.org/10.1039/C7EM00419B
1166 Kothawala, D. N., Watmough, S. A., Futter, M. N., Zhang, L., & Dillon, P. J. (2011). Stream
1167 Nitrate Responds Rapidly to Decreasing Nitrate Deposition. *Ecosystems*, *14*(2), 274–286.
1168 https://doi.org/10.1007/s10021-011-9422-1
1169 Lawrence, G. B., Scanga, S. E., & Sabo, R. D. (2020). Recovery of Soils From Acidic
1170 Deposition May Exacerbate Nitrogen Export From Forested Watersheds. *Journal of*
1171 *Geophysical Research: Biogeosciences*, *125*(1). https://doi.org/10.1029/2019JG005036
1172 Li, Y., Schichtel, B. A., Walker, J. T., Schwede, D. B., Chen, X., Lehmann, C. M. B., et al.
1173 (2016). Increasing importance of deposition of reduced nitrogen in the United States.
1174 *Proceedings of the National Academy of Sciences*, *113*(21), 5874–5879.
1175 https://doi.org/10.1073/pnas.1525736113
1176 Lovett, G. M., & Goodale, C. L. (2011). A New Conceptual Model of Nitrogen Saturation Based
1177 on Experimental Nitrogen Addition to an Oak Forest. *Ecosystems*, *14*(4), 615–631.
1178 https://doi.org/10.1007/s10021-011-9432-z

1179 Lovett, G. M., Weathers, K. C., & Sobczak, W. V. (2000). Nitrogen Saturation and Retention in
1180 the Forested Watersheds of the Catskill Mountains, New York. *Ecological Applications*,
1181 *10*(1), 73–84. https://doi.org/10.1890/1051-0761(2000)010[0073:NSARIF]2.0.CO;2
1182 Lovett, G. M., Goodale, C. L., Ollinger, S. V., Fuss, C. B., Ouimette, A. P., & Likens, G. E.
1183 (2018). Nutrient retention during ecosystem succession: a revised conceptual model.
1184 *Frontiers in Ecology and the Environment*, *16*(9), 532–538.
1185 https://doi.org/10.1002/fee.1949
1186 Lucas, R. W., Klaminder, J., Futter, M. N., Bishop, K. H., Egnell, G., Laudon, H., & Högberg, P.
1187 (2011). A meta-analysis of the effects of nitrogen additions on base cations: Implications
1188 for plants, soils, and streams. *Forest Ecology and Management*, *262*(2), 95–104.
1189 https://doi.org/10.1016/j.foreco.2011.03.018
1190 Lucas, R. W., Sponseller, R. A., Gundale, M. J., Stendahl, J., Fridman, J., Högberg, P., &
1191 Laudon, H. (2016). Long-term declines in stream and river inorganic nitrogen (N) export
1192 correspond to forest change. *Ecological Applications*, *26*(2), 545–556.
1193 https://doi.org/10.1890/14-2413
1194 Maavara, T., Lauerwald, R., Laruelle, G. G., Akbarzadeh, Z., Bouskill, N. J., Van Cappellen, P.,
1195 & Regnier, P. (2019). Nitrous oxide emissions from inland waters: Are IPCC estimates
1196 too high? *Global Change Biology*, *25*(2), 473–488. https://doi.org/10.1111/gcb.14504
1197 Marinos, R. E., Campbell, J. L., Driscoll, C. T., Likens, G. E., McDowell, W. H., Rosi, E. J., et
1198 al. (2018). Give and Take: A Watershed Acid Rain Mitigation Experiment Increases
1199 Baseflow Nitrogen Retention but Increases Stormflow Nitrogen Export. *Environmental*
1200 *Science & Technology*, *52*(22), 13155–13165. https://doi.org/10.1021/acs.est.8b03553

1201 Maurer, E. P. (2016). CONUS digital elevation model of 1/16 degree grid cells. Retrieved from
1202 https://www.hydroshare.org/resource/c18cef883695498c81acf9c4260d1e53/
1203 Maurer, E. P., Lettenmaier, D. P., & Mantua, N. J. (2004). Variability and potential sources of
1204 predictability of North American runoff. *Water Resources Research*, *40*(9).
1205 https://doi.org/10.1029/2003WR002789
1206 Moatar, F., Abbott, B. W., Minaudo, C., Curie, F., & Pinay, G. (2017). Elemental properties,
1207 hydrology, and biology interact to shape concentration-discharge curves for carbon,
1208 nutrients, sediment, and major ions: SHAPES AND CAUSES OF C-Q
1209 RELATIONSHIPS. *Water Resources Research*, *53*(2), 1270–1287.
1210 https://doi.org/10.1002/2016WR019635
1211 Monteith, D. T., Stoddard, J. L., Evans, C. D., de Wit, H. A., Forsius, M., Høgåsen, T., et al.
1212 (2007). Dissolved organic carbon trends resulting from changes in atmospheric
1213 deposition chemistry. *Nature*, *450*(7169), 537–540. https://doi.org/10.1038/nature06316
1214 Moritz, S., Sardá, A., Bartz-Beielstein, T., Zaefferer, M., & Stork, J. (2015). Comparison of
1215 different Methods for Univariate Time Series Imputation in R. *ArXiv:1510.03924 [Cs, Stat]*. Retrieved from http://arxiv.org/abs/1510.03924
1217 MRLC NLCD. (2020). NLCD Land Cover Change Index (CONUS) Multi-Resolution Land
1218 Characteristics (MRLC) consortium National Land Cover Database. Land Cover Change
1219 Index. Retrieved from https://www.mrlc.gov/data/nlcd-land-cover-change-index-conus
1220 Mulholland, P. J., Hall, R. O., Sobota, D. J., Dodds, W. K., Findlay, S. E. G., Grimm, N. B., et
1221 al. (2009). Nitrate removal in stream ecosystems measured by 15N addition experiments:
1222 Denitrification. *Limnology and Oceanography*, *54*(3), 666–680.
1223 https://doi.org/10.4319/lo.2009.54.3.0666

1224 Murphy, J., & Sprague, L. (2019). Water-quality trends in US rivers: Exploring effects from
1225 streamflow trends and changes in watershed management. *Science of The Total*
1226 *Environment*, *656*, 645–658. https://doi.org/10.1016/j.scitotenv.2018.11.255
1227 Murphy, S. F., Writer, J. H., McCleskey, R. B., & Martin, D. A. (2015). The role of precipitation
1228 type, intensity, and spatial distribution in source water quality after wildfire.
1229 *Environmental Research Letters*, *10*(8), 084007. https://doi.org/10.1088/1748-
1230 9326/10/8/084007
1231 Musolff, A., Schmidt, C., Selle, B., & Fleckenstein, J. H. (2015). Catchment controls on solute
1232 export. *Advances in Water Resources*, *86*, 133–146.
1233 https://doi.org/10.1016/j.advwatres.2015.09.026
1234 Musolff, A., Schmidt, C., Rode, M., Lischeid, G., Weise, S. M., & Fleckenstein, J. H. (2016).
1235 Groundwater head controls nitrate export from an agricultural lowland catchment.
1236 *Advances in Water Resources*, *96*, 95–107.
1237 https://doi.org/10.1016/j.advwatres.2016.07.003
1238 Musolff, A., Selle, B., Büttner, O., Opitz, M., & Tittel, J. (2017). Unexpected release of
1239 phosphate and organic carbon to streams linked to declining nitrogen depositions. *Global*
1240 *Change Biology*, *23*(5), 1891–1901. https://doi.org/10.1111/gcb.13498
1241 NADP. (2018). National Atmospheric Deposition Program (NRSP-3). NADP Program Office,
1242 Wisconsin State Laboratory of Hygiene, 465 Henry Mall, Madison, WI 53706. Retrieved
1243 October 24, 2018, from http://nadp.slh.wisc.edu/committees/tdep/tdepmaps/
1244 Newcomer, M. E., Hubbard, S. S., Fleckenstein, J. H., Maier, U., Schmidt, C., Thullner, M., et
1245 al. (2018). Influence of Hydrological Perturbations and Riverbed Sediment

1246 Characteristics on Hyporheic Zone Respiration of CO_2 and N_2. *Journal of Geophysical*
1247 *Research: Biogeosciences*, *123*(3), 902–922. https://doi.org/10.1002/2017JG004090
1248 O'Donnell, J. A., Aiken, G. R., Kane, E. S., & Jones, J. B. (2010). Source water controls on the
1249 character and origin of dissolved organic matter in streams of the Yukon River basin,
1250 Alaska. *Journal of Geophysical Research*, *115*(G3).
1251 https://doi.org/10.1029/2009JG001153
1252 Oelsner, G. P., & Stets, E. G. (2019). Recent trends in nutrient and sediment loading to coastal
1253 areas of the conterminous U.S.: Insights and global context. *Science of The Total*
1254 *Environment*, *654*, 1225–1240. https://doi.org/10.1016/j.scitotenv.2018.10.437
1255 Oelsner, G. P., Sprague, L. A., Murphy, J. C., Zuellig, R. E., Johnson, H. M., Ryberg, K. R., et
1256 al. (2017). *Water-quality trends in the Nation's rivers and streams, 1972–2012—Data*
1257 *preparation, statistical methods, and trend results (ver. 2.0, October 2017)* (Scientific
1258 Investigations Report No. U.S. Geological Survey Scientific Investigations Report 2017–
1259 5006) (p. 136). U.S. Geological Survey. Retrieved from
1260 https://doi.org/10.3133/sir20175006
1261 Pardo, L. H., Fenn, M. E., Goodale, C. L., Geiser, L. H., Driscoll, C. T., Allen, E. B., et al.
1262 (2011). Effects of nitrogen deposition and empirical nitrogen critical loads for ecoregions
1263 of the United States. *Ecological Applications*, *21*(8), 3049–3082.
1264 https://doi.org/10.1890/10-2341.1
1265 Pellerin, B. A., Bergamaschi, B. A., Gilliom, R. J., Crawford, C. G., Saraceno, J., Frederick, C.
1266 P., et al. (2014). Mississippi River Nitrate Loads from High Frequency Sensor
1267 Measurements and Regression-Based Load Estimation. *Environmental Science &*
1268 *Technology*, *48*(21), 12612–12619. https://doi.org/10.1021/es504029c

1269 Pinder, R. W., Davidson, E. A., Goodale, C. L., Greaver, T. L., Herrick, J. D., & Liu, L. (2012).
1270 Climate change impacts of US reactive nitrogen. *Proceedings of the National Academy of*
1271 *Sciences*, *109*(20), 7671–7675. https://doi.org/10.1073/pnas.1114243109
1272 Quilbé, R., Rousseau, A. N., Duchemin, M., Poulin, A., Gangbazo, G., & Villeneuve, J.-P.
1273 (2006). Selecting a calculation method to estimate sediment and nutrient loads in streams:
1274 Application to the Beaurivage River (Québec, Canada). *Journal of Hydrology*, *326*(1–4),
1275 295–310. https://doi.org/10.1016/j.jhydrol.2005.11.008
1276 R Core Team. (2014). R: A language and environment for statistical computing. Retrieved from
1277 http://www.R-project.org/.
1278 Read, E. K., Carr, L., De Cicco, L., Dugan, H. A., Hanson, P. C., Hart, J. A., et al. (2017). Water
1279 quality data for national-scale aquatic research: The Water Quality Portal. *Water*
1280 *Resources Research*, *53*(2), 1735–1745. https://doi.org/10.1002/2016WR019993
1281 Renwick, W. H., Vanni, M. J., Fisher, T. J., & Morris, E. L. (2018). Stream Nitrogen,
1282 Phosphorus, and Sediment Concentrations Show Contrasting Long-term Trends
1283 Associated with Agricultural Change. *Journal of Environmental Quality*, *47*(6), 1513–
1284 1521. https://doi.org/10.2134/jeq2018.04.0162
1285 Rhoades, C. C., Hubbard, R. M., & Elder, K. (2017). A Decade of Streamwater Nitrogen and
1286 Forest Dynamics after a Mountain Pine Beetle Outbreak at the Fraser Experimental
1287 Forest, Colorado. *Ecosystems*, *20*(2), 380–392. https://doi.org/10.1007/s10021-016-0027-
1288 6
1289 Rhoades, C. C., Chow, A. T., Covino, T. P., Fegel, T. S., Pierson, D. N., & Rhea, A. E. (2018).
1290 The Legacy of a Severe Wildfire on Stream Nitrogen and Carbon in Headwater
1291 Catchments. *Ecosystems*. https://doi.org/10.1007/s10021-018-0293-6

1292 SanClements, M. D., Fernandez, I. J., Lee, R. H., Roberti, J. A., Adams, M. B., Rue, G. A., &
1293 McKnight, D. M. (2018). Long-Term Experimental Acidification Drives Watershed
1294 Scale Shift in Dissolved Organic Matter Composition and Flux. *Environmental Science &*
1295 *Technology*, *52*(5), 2649–2657. https://doi.org/10.1021/acs.est.7b04499
1296 Schwede, D. B., & Lear, G. G. (2014). A novel hybrid approach for estimating total deposition in
1297 the United States. *Atmospheric Environment*, *92*, 207–220.
1298 https://doi.org/10.1016/j.atmosenv.2014.04.008
1299 Seaber, P. R., Kapinos, F. P., & Knapp, G. L. (1987). *Hydrologic Unit Maps* (USGS Water
1300 Supply Paper No. Water-Supply Paper 2294) (p. 63). U.S. Geological Survey. Retrieved
1301 from https://water.usgs.gov/GIS/huc.html
1302 Seitzinger, S., Harrison, J. A., Böhlke, J. K., Bouwman, A. F., Lowrance, R., Peterson, B., et al.
1303 (2006). Denitrifcation Across Landscapes and Watersheds: A Synthesis. *Ecological*
1304 *Applications*, *16*(6), 2064–2090. https://doi.org/10.1890/1051-
1305 0761(2006)016[2064:DALAWA]2.0.CO;2
1306 Shoda, M. E., Sprague, L. A., Murphy, J. C., & Riskin, M. L. (2019). Water-quality trends in
1307 U.S. rivers, 2002 to 2012: Relations to levels of concern. *Science of The Total*
1308 *Environment*, *650*, 2314–2324. https://doi.org/10.1016/j.scitotenv.2018.09.377
1309 Shultz, M., Pellerin, B., Aiken, G., Martin, J., & Raymond, P. (2018). High Frequency Data
1310 Exposes Nonlinear Seasonal Controls on Dissolved Organic Matter in a Large
1311 Watershed. *Environmental Science & Technology*, *52*(10), 5644–5652.
1312 https://doi.org/10.1021/acs.est.7b04579

1313 Sinha, E., & Michalak, A. M. (2016). Precipitation Dominates Interannual Variability of
1314 Riverine Nitrogen Loading across the Continental United States. *Environmental Science*
1315 *& Technology*, *50*(23), 12874–12884. https://doi.org/10.1021/acs.est.6b04455
1316 Smith, R. A., Alexander, R. B., & Wolman, M. G. (1987). Water-Quality Trends in the Nation's
1317 Rivers. *Science*, *235*(4796), 1607–1615. https://doi.org/10.1126/science.235.4796.1607
1318 Spruce, J. P., Gasser, G. E., & Hargrove, W. W. (2016). MODIS NDVI Data, Smoothed and
1319 Gap-filled, for the Conterminous US: 2000-2015. ORNL Distributed Active Archive
1320 Center. https://doi.org/10.3334/ORNLDAAC/1299
1321 Stegen, J. C., Johnson, T., Fredrickson, J. K., Wilkins, M. J., Konopka, A. E., Nelson, W. C., et
1322 al. (2018). Influences of organic carbon speciation on hyporheic corridor
1323 biogeochemistry and microbial ecology. *Nature Communications*, *9*(1), 585.
1324 https://doi.org/10.1038/s41467-018-02922-9
1325 Stoddard, J. L. (1994). Long-Term Changes in Watershed Retention of Nitrogen: Its Causes and
1326 Aquatic Consequences. In L. A. Baker (Ed.), *Environmental Chemistry of Lakes and*
1327 *Reservoirs* (Vol. 237, pp. 223–284). Washington, DC: American Chemical Society.
1328 https://doi.org/10.1021/ba-1994-0237.ch008
1329 Stoddard, J. L., Jeffries, D. S., Lükewille, A., Clair, T. A., Dillon, P. J., Driscoll, C. T., et al.
1330 (1999). Regional trends in aquatic recovery from acidification in North America and
1331 Europe. *Nature*, *401*(6753), 575–578. https://doi.org/10.1038/44114
1332 Stoddard, J. L., Van Sickle, J., Herlihy, A. T., Brahney, J., Paulsen, S., Peck, D. V., et al. (2016).
1333 Continental-Scale Increase in Lake and Stream Phosphorus: Are Oligotrophic Systems
1334 Disappearing in the United States? *Environmental Science & Technology*, *50*(7), 3409–
1335 3415. https://doi.org/10.1021/acs.est.5b05950

1336 Sudduth, E. B., Perakis, S. S., & Bernhardt, E. S. (2013). Nitrate in watersheds: Straight from
1337 soils to streams. *Journal of Geophysical Research: Biogeosciences*, *118*(1), 291–302.
1338 https://doi.org/10.1002/jgrg.20030
1339 Terrer, C., Vicca, S., Stocker, B. D., Hungate, B. A., Phillips, R. P., Reich, P. B., et al. (2018).
1340 Ecosystem responses to elevated CO_2 governed by plant-soil interactions and the cost of
1341 nitrogen acquisition. *New Phytologist*, *217*(2), 507–522.
1342 https://doi.org/10.1111/nph.14872
1343 USGS. (2016). USGS NWIS Station Mapper. Retrieved from
1344 http://maps.waterdata.usgs.gov/mapper/index.html
1345 USGS. (2018). National Water Information System-Web Interface. Retrieved from
1346 https://waterdata.usgs.gov/nwis
1347 Van Breemen, N., Boyer, E. W., Goodale, C. L., Jaworski, N. A., Paustian, K., Seitzinger, S. P.,
1348 et al. (2002). Where Did All the Nitrogen Go? Fate of Nitrogen Inputs to Large
1349 Watersheds in the Northeastern U.S.A. *Biogeochemistry*, *57/58*, 267–293.
1350 Van Meter, K. J., & Basu, N. B. (2015). Catchment Legacies and Time Lags: A Parsimonious
1351 Watershed Model to Predict the Effects of Legacy Storage on Nitrogen Export. *PLOS*
1352 *ONE*, *10*(5), e0125971. https://doi.org/10.1371/journal.pone.0125971
1353 Van Meter, K. J., & Basu, N. B. (2017). Time lags in watershed-scale nutrient transport: an
1354 exploration of dominant controls. *Environmental Research Letters*, *12*(8), 084017.
1355 https://doi.org/10.1088/1748-9326/aa7bf4
1356 Van Meter, K. J., Basu, N. B., Veenstra, J. J., & Burras, C. L. (2016). The nitrogen legacy:
1357 emerging evidence of nitrogen accumulation in anthropogenic landscapes. *Environmental*
1358 *Research Letters*, *11*(3), 035014. https://doi.org/10.1088/1748-9326/11/3/035014

1359 Vitousek, P. M., & Reiners, W. A. (1975). Ecosystem Succession and Nutrient Retention: A
1360 Hypothesis. *BioScience*, *25*(6), 376–381. https://doi.org/10.2307/1297148
1361 Vuorenmaa, J., Augustaitis, A., Beudert, B., Bochenek, W., Clarke, N., de Wit, H. A., et al.
1362 (2018). Long-term changes (1990–2015) in the atmospheric deposition and runoff water
1363 chemistry of sulphate, inorganic nitrogen and acidity for forested catchments in Europe in
1364 relation to changes in emissions and hydrometeorological conditions. *Science of The*
1365 *Total Environment*, *625*, 1129–1145. https://doi.org/10.1016/j.scitotenv.2017.12.245
1366 Wasserstein, R. L., & Lazar, N. A. (2016). The ASA Statement on *p* -Values: Context, Process,
1367 and Purpose. *The American Statistician*, *70*(2), 129–133.
1368 https://doi.org/10.1080/00031305.2016.1154108
1369 Yanai, R. D., Vadeboncoeur, M. A., Hamburg, S. P., Arthur, M. A., Fuss, C. B., Groffman, P.
1370 M., et al. (2013). From Missing Source to Missing Sink: Long-Term Changes in the
1371 Nitrogen Budget of a Northern Hardwood Forest. *Environmental Science & Technology*,
1372 *47*(20), 11440–11448. https://doi.org/10.1021/es4025723
1373 Yang, L., Jin, S., Danielson, P., Homer, C., Gass, L., Bender, S. M., et al. (2018). A new
1374 generation of the United States National Land Cover Database: Requirements, research
1375 priorities, design, and implementation strategies. *ISPRS Journal of Photogrammetry and*
1376 *Remote Sensing*, *146*, 108–123. https://doi.org/10.1016/j.isprsjprs.2018.09.006
1377 Zarnetske, J. P., Bouda, M., Abbott, B. W., Saiers, J., & Raymond, P. A. (2018). Generality of
1378 Hydrologic Transport Limitation of Watershed Organic Carbon Flux Across Ecoregions
1379 of the United States. *Geophysical Research Letters*, *45*(21), 11,702-11,711.
1380 https://doi.org/10.1029/2018GL080005
1381

1382